

# UC San Diego

## UC San Diego Electronic Theses and Dissertations

### Title

PPAR[delta] activation enhances skeletal muscle regeneration

### Permalink

<https://escholarship.org/uc/item/3vq8k734>

### Author

Embler, Emi Kanakubo

### Publication Date

2012

Peer reviewed|Thesis/dissertation

UNIVERSITY OF CALIFORNIA, SAN DIEGO

PPARdelta activation enhances skeletal muscle regeneration

A dissertation submitted in partial satisfaction of the requirements for the degree of  
Doctor of Philosophy

in

Biology

by

Emi Kanakubo Embler

Committee in charge:

Professor Ronald M. Evans, Chair  
Professor Andrew Dillin  
Professor Christopher Glass  
Professor Amy Kiger  
Professor Richard Lieber

2012

Copyright

Emi Kanakubo Embler, 2012

All rights reserved

The dissertation of Emi Kanakubo Embler is approved, and it is acceptable in quality and form for publication on microfilm and electronically:

---

---

---

---

---

Chair

UNIVERSITY OF CALIFORNIA, SAN DIEGO

2012

# DEDICATION

いつでも、いつまでも、私をサポートしてくれる両親に  
この卒業論文を捧げます。

パパとお母さんの協力と後押しがあったから、大きな壁を  
乗り越えられました。心から感謝しています。

# TABLE OF CONTENTS

SIGNATURE PAGE.....	iii
DEDICATION .....	iv
TABLE OF CONTENTS .....	v
LIST OF ABBREVIATIONS .....	vi
LIST OF FIGURES AND TABLES .....	vii
ACKNOWLEDGEMENTS .....	ix
VITA.....	xi
ABSTRACT OF THE DISSERTATION.....	xii
Chapter 1: Introduction.....	1
Chapter 2: Effects of muscle specific activation of PPARdelta during skeletal muscle regeneration after acute injury .....	18
Chapter 3: Effects of pharmacological activation of PPARdelta during skeletal muscle regeneration after acute injury .....	56
Chapter 4: Conclusions.....	76

# LIST OF ABBREVIATIONS

PPAR $\delta$ .....	Peroxisome Proliferator-Activated Receptor delta
TG.....	Transgenic
WT.....	Wildtype
KO.....	Knock-out
TA.....	Tibialis Anterior
Gastroc.....	Gastrocnemius
Sol.....	Soleus
uninj.....	Uninjured
inj.....	Injured
GW.....	GW501516
Ctrl.....	Control
Veh.....	Vehicle
DMSO.....	Dimethyl Sulfoxide
EBD.....	Evans Blue Dye
IP.....	Intraperitoneal
H&E.....	Hematoxylin and Eosin

# LIST OF FIGURES AND TABLES

Figure 1.2: Nuclear receptor binding DNA motifs.....	11
Figure 1.3: Schematic representation of the functional domains of PPARdelta .....	12
Figure 2.1: VP16-PPARdelta animals show increased efficiency in restoration of fiber integrity after injury. ....	40
Figure 2.2: Skeletal muscle specific activation of PPARdelta expedites regenerative process after acute injury.....	41
Figure 2.3: GO analysis of up-regulated genes in TG compared to WT in response to acute thermal injury.....	42
Table 2.1: List of notable up-regulated genes in injured TG compared to WT from microarray analyses of 3 days post injury TA.....	43
Figure 2.4: PPAR $\delta$ activation leads to temporal shift, thus increased efficiency, of the regenerative process. ....	44
Figure 2.5: Muscle specific activation of PPAR $\delta$ increases quiescent satellite cell population.....	45
Figure 2.6: PPAR $\delta$ activation augments myoblast proliferation after the injury.....	46
Figure 2.7: Transgene is not expressed in the satellite cells.....	47
Figure 2.8: PPAR $\delta$ activation induces increase in vascularity.....	48
Figure 3.1: Oral administration of GW501516 induces expression of PPAR $\delta$ target genes in quadriceps.....	70
Figure 3.2: GW501516 treatment expedites restoration of fiber integrity after thermal injury.....	71



Figure 3.3: GW501516 treatment promotes resolution of inflammatory response..... 72

Figure 3.4: GW501516 treatment enhances proliferation of myoblasts after the injury.  
..... 73

Figure 3.5: GW501516 treatment activates Notch1 signaling pathway..... 74

# ACKNOWLEDGEMENTS

First, I would like to thank my advisor, Ron Evans, for an awesome graduate school experience. It was not always an easy ride, but the lab was always a place I wanted to be. I am forever grateful for the opportunity.

I was very lucky to be surrounded by great people in the Evans lab. In particular, Dr. Vihang Narkar, who as my rotation supervisor, started it all. I thank Dr. Michael Downes and Dr. Annette Atkins for their kindness and moral support through all the rocky patches. I would like to acknowledge Dr. Yasuyuki Kida and Dr. Suk Hyun Hong for day to day scientific and personal discussions. Thanks to my friends in the Evans lab, Dr. Li Tai, Jackie Alvarez, Sandra Jacinto, Ester Banayo, Ling Chong and Samantha Kaufman. I thank Sally Ganley for facilitating the impossible, namely getting my committee members together and scheduling meetings with Ron. Lastly, I would like to thank Lita Ong for good gossips and her unique ways – but most of all, for her continuing support and encouragement, personally and scholastically.

I attribute great part of my success in graduate school to the support from my family. Jon has made numerous sacrifices during the past several years, and I feel grateful and lucky to have a partner who allows me to be me and not me, when I'm being crazy.

Chapters 2 and 3, in parts, are currently being prepared for submission for publication. Embler, EK; Atkins, A; Downes, M; Evans RM. The dissertation author was the primary investigator and author of this material.

# VITA

- 2001 Bachelor of Science, Massachusetts Institute of Technology
- 2012 Doctor of Philosophy, University of California, San Diego

## PUBLICATIONS

Narkar V.A., Downes M., Yu R.T., **Embler E.**, Wang Y.X., Banayo E., Mihaylova M.M., Nelson M.C., Zou Y., Juguilon H., Kang H., Shaw R.J., and R.M. Evans. "AMPK and PPARdelta agonists are exercise mimetics." *Cell*. 134(3): 405-15, 2008.

Samoszuk M., **Kanakubo E.**, and J.K. Chan. "Degranulating mast cells in fibrotic regions of human tumors and evidence that mast cell heparin interferes with the growth of tumor cells through a mechanism involving fibroblasts." *BMC Cancer*. 5: 121, 2005.

Nie Z., Yan Z., Chen E.H., Sechi S., Ling C., Zhou S., Xue Y., Yang D., Murray D., **Kanakubo E.**, Cleary M.L., and W. Wang. "Novel SWI/SNF chromatin-remodeling complexes contain a mixed-lineage leukemia chromosomal translocation partner." *Mol Cell Biol*. 23(8): 2942-52, 2003.

Yasuhara S., Perez M.E., **Kanakubo E.**, Yasuhara Y., Shin Y.S., Kaneki M., Fujita T., and J.A. Martyn. "Skeletal muscle apoptosis after burns is associated with activation of proapoptotic signals." *Am J Physiol Endocrinol Metab*. 279(5): E1114-21, 2000.

Yasuhara S., **Kanakubo E.**, Perez M.E., Kaneki M., Fujita T., Okamaoto T., and J.A. Martyn. "Burn injury induces skeletal muscle apoptosis and the activation of caspase pathways in rats." *J Burn Care Rehabil*. 20(6): 462-70, 1999.

ABSTRACT OF THE DISSERTATION

PPARdelta activation enhances skeletal muscle regeneration

by

Emi Kanakubo Embler

Doctor of Philosophy in Biology

University of California, San Diego, 2012

Professor Ronald M. Evans, Chair

Skeletal muscle relies mostly on its resident progenitor cells, the satellite cells, for postnatal growth and regeneration. Therefore, maintaining proper function and healthy population of satellite cells are critical for the ability of muscle to control damage. Endurance exercise elicits a myriad of adaptive responses in the muscle, including an increase in the satellite cell number. Targeted expression of constitutively active Peroxisome Proliferator-Activated Receptor delta (VP16-PPAR $\delta$ ) in the skeletal muscle mimics endurance training induced fiber type remodeling,

including, glycolytic to oxidative fiber type switch and concomitant increase in the running capacity. Currently, however, it is unknown whether transcriptionally directed “endurance exercise training” adaptations by PPAR $\delta$  in the muscle is sufficient to affect satellite cell homeostasis and function. We herein present that PPAR $\delta$  activation promotes acceleration of regenerative process after an acute injury. We found that the skeletal muscle specific over-expression of PPAR $\delta$  induces increase in the satellite cell population. Furthermore, we observed an increase in the number of proliferating cells after injury, leading to an increase in the number of nascent regenerating fibers. Gene expression analyses showed an earlier resolution of inflammatory response and induction of myogenic markers, suggesting that PPAR $\delta$  actuates temporal shift of the regenerative process. Interestingly, PPAR $\delta$  promotes myoblast proliferation immediately after the injury, which correlates with strong induction of Notch signaling pathway by PPAR $\delta$ . Additionally, acute pharmacological activation of PPAR $\delta$  also promoted efficient restoration of fiber integrity. Collectively, our results demonstrate a new role for PPAR $\delta$  in skeletal muscle regeneration. Our findings allude to the therapeutic potential of PPAR $\delta$ , not only for the treatment of an acute injury, but also in Notch-dependent aging associated loss of regenerative capacity of the muscle.

**Chapter 1:**  
**Introduction**

Skeletal muscle fiber is a multinucleated syncytia and constitutes a single cell unit of the muscle. Diversity of fiber types in their metabolic and contractile properties allows for the plasticity of skeletal muscles to adapt to the changing demands of the body. Myofibers can be characterized by their expression of myosin heavy chain (MHC) isoforms. Myofibers express either type I or II MHC isoforms, where type II is further subdivided into a, b and x based on their metabolic properties, where type IIa fibers are fast oxidative and type IIb are fast glycolytic and type IIx lying in between. Type I fibers have slow peak to tension time and utilizes oxidative metabolism, whereas type II fibers have fast peak to tension time and metabolically glycolytic (Zierath and Hawley, 2004). The heterogeneity of fiber types allows for a wide range of metabolic and mechanical output.

Skeletal muscles are adaptable to meet the demands of the body. For example, exercise induces fiber type transitions in skeletal muscles (Bassel-Duby, 2006). Exercise can largely be classified into two major subtypes: resistance and endurance. Both types of exercise elicit profound changes in skeletal muscle, but through different molecular mechanisms (Baar, 2006). Resistance exercise has been shown to induce hypertrophy via increased protein synthesis (MacDougall, 1995). Correspondingly, hallmarks of endurance exercise are increased mitochondrial mass, oxidative enzymes, and slow twitch proteins, decreased glycolytic proteins and hypotrophy in fast twitch fibers (Baar, 2006). Resistance exercise has been shown to inflict damage to the muscle by permeabilization of tissue and subsequent hyperemia (Vierck, 2000; Darr, 1987). This enables the influx of soluble factors, presumably leading to the activation of satellite cells. In rats, endurance training has also been shown to increase satellite



cell number (Umnova, 1991). Also in rats, fast to slow fiber type switch induced by chronic low frequency electric stimulation, is inhibited by ablation of satellite cells by  $\gamma$  irradiation (Martins, 2006). These findings demonstrate that the skeletal muscle remodeling in adult animals are mediated by satellite cells. It is unclear whether in managing exercise induced adaptations in skeletal muscles, contributions from satellite cells are solicited in the absence of damage to the fibers.

Alexander Mauro first described satellite cells based on their unique habitat within a myofiber: they are “wedged” between the basement membrane and the plasma membrane of a myofiber (Mauro, 1961). Seminal findings came in the 1970s, which brought satellite cells into the limelight. In 1971, Moss and Leblond demonstrated proliferation and fusion capacity of satellite cells using single-injection  $^3\text{H}$ -thymidine labeling in the tibialis anterior muscle of growing (young) rats (Moss, 1970). A few years later, Schultz et al. used continuous infusion of  $^3\text{H}$ -thymidine to show that the majority of satellite cells in non-growing (adult) mice are mitotically quiescent (Schultz, 1978). Around the same time, M.H. Snow showed that transplantation of minced  $^3\text{H}$ -thymidine labeled triceps muscle into extirpated triceps of unlabeled littermate is able to reconstitute injured host myofibers (Snow, 1978). Collectively, these findings steered toward the view that the satellite cells are a distinct population of cells residing on the periphery of myofibers and contributing to the growth and regeneration of skeletal muscles. Over 40 years after the initial observations by Mauro, the “stemness,” origin and identity of satellite cells have continuously been scrutinized. Presently, satellite cells are best classified as myogenic progenitors. Their self-renewal and differentiation capacity have alluded to the

archetypic “stemness,” but their fate seems largely committed (Sinanan,2006; Beauchamp, 2000).

Developmentally, satellite cells originate from the somites (Schienda, 2005; Gros, 2005). In vertebrates, paraxial mesoderm undergoes segmentation to form somites, which then compartmentalize into sclerotome and dermomyotome (Christ, 1995). Muscle progenitor cells delaminate from hypaxial dermomyotome and migrate and proliferate to form muscle masses in putative limbs (Relaix, 2004). These developmental processes, propagated by the interplay between mesenchymal cells and their surroundings, are mediated by various regulatory factors. Pax3, and its target gene *c-met*, are critical during early stages of myogenesis (Shi, 2006). Mice with homozygous mutation in Pax3 gene are embryonic lethal and show significant defect in neural tube and neural crest cell formation as well as somitic defects, resulting in a complete lack of limb muscles (Bober, 1994). Expression of Pax3 is first detected in presomitic mesoderm, and persists through to the somitic epithelium of the dermomyotome (Relaix, 2005; Goulding, 1991). Pax7 is detected in central dermomyotome (Relaix, 2004). Subsequently in the myotome, about 87% of the cells are Pax3<sup>+</sup>Pax7<sup>+</sup> (Relaix, 2005). Subpopulation of these Pax3<sup>+</sup>Pax7<sup>+</sup> cells are believed to persist through development without entering myogenic program, and later exhibit the properties of satellite cells (Schienda, 2005; Gros, 2005; Relaix, 2005). Pax7, a paralogue of Pax3, has been shown to be indispensable for a complete myogenesis. Initially, Pax7<sup>-/-</sup> mice were reported to suffer from cephalic neural crest defects, exhibiting malformations of cranial structures and succumbing to premature death at a mere 2 weeks of age (Mansouri, 1996). Notably, the authors of this report

observed no obvious phenotype in skeletal muscle, such that embryonic and fetal myogenesis produced architecturally sound skeletal muscles (Mansouri, 1996). Beyond the obvious, however, Pax7<sup>-/-</sup> mice are completely devoid of satellite cells, thus unable to sustain postnatal growth of musculature, exhibiting growth retardation (Seale, 2000).

Aside from their classical definition based on their sublaminar positioning, efforts to identify satellite cells by a unique set of markers have led to the idea of phenotypic and functional heterogeneity amongst the cells residing in the satellite cell compartment (Mauro, 1961; Sinanan, 2006; Wagers, 2005; Peault, 2007; Dhawan, 2005). Physical infiltration of the satellite cell compartment by hematopoietic cells in response to damage has been documented (Wagers, 2005). Albeit at low frequency, skeletal muscle harbors a variety of cell types, including side population (SP) cells, “muscle-derived stem cells” (MDSC) or “multipotent adult progenitor cells” (MAPC), mesenchymal stem cells (MSC), and mesoangioblasts (Sinanan, 2006; Wagers, 2005; Dellavalle, 2007; Peault, 2007). They are known to possess multipotency, however, their contributions in muscle regeneration are considered insignificant compared to that of satellite cells (Collins, 2005; Sherwood, 2004). Functionally, a small portion of satellite cells has been shown to exhibit a distinctively slower rate of proliferation (Schultz, 1996). Additionally, dynamics of their cellular states may contribute to the appearance of heterogeneity of the satellite cell population. Commonly, satellite cells are extracted from tissue by enzymatic digestion and enriched by cell sorting based on cell-surface markers. However, satellite cells are highly prone to activation upon extraction from their niche – hence, change in cellular states. Currently, most

quiescent satellite cells are identified by the expressions of Pax7, M-Cadherin, CD34, and Myf5 (Beauchamp, 2000; Seale, 2000; Irintchev, 1994). It has also been reported that a novel antibody, SM/C-2.6, detects a unique epitope expressed by the quiescent satellite cells (Fukuda, 2004).

Perxisome Proliferator-Activated Receptors (PPAR) are ligand-dependent nuclear transcription factors that belong to group C in superfamily of nuclear hormone receptors (Nuclear Receptor Nomenclature Committee, 1999). To date, there are 48 members of the nuclear hormone receptor superfamily in humans and 49 members in mice (Figure 1.1) (Bookout, 2006). The PPARs were named based on the discovery of PPAR $\alpha$ , which was shown to be activated by hepatocarcinogens that cause proliferation of peroxisomes (Issemann, 1990). Shortly thereafter, two more isoforms,  $\gamma$ , and  $\beta/\delta$ , were found, and together, they came to be referred to as the PPAR family (Laudet, 2002). PPARs form obligatory heterodimers with retinoid X receptor (RXR) and bind to peroxisome proliferator response elements (PPREs) of their target genes to initiate transcription upon ligand binding (Kliewer, 1992). PPRE is a characteristic DR-1 motif, where two direct repeats of consensus sequence AGGTCA is separated by a single nucleotide (Figure 1.2) (Kliewer, 1992). PPARs have the typical modular structure of nuclear receptors (Figure 1.3) The least conserved domain between the three PPAR isoforms is the N-terminal ligand-independent transactivation domain, followed by the most similar DNA binding domain. The hinge region is critical for structural characteristics of the nuclear receptors and also accepts interactions with cofactors (Dowell, 1997; Iwata, 2001; Tomaru, 2006). Ligand binding domain serves

as a platform for heterodimerization with RXR and interactions with coactivators (Nolte, 1998; Schulman, 1998). The LBD of PPARs is hydrophobic, large Y-shaped cavity with a flexible entrance, which allows for accepting a variety of endogenous and synthetic lipophilic ligands (Ehrenborg, 2009).

PPAR $\alpha$  is predominantly expressed in the liver, PPAR $\gamma$  I abundant in adipose tissues and PPAR $\delta$  is ubiquitously expressed albeit at low levels in the liver (Chawla, 1994; Kliewer, 1994; Issemann, 1990). They serve as lipid sensors of the body and as such, bind to and are activated by dietary fatty acids and their derivatives in order to transcriptionally regulate lipid homeostasis in the body (Barish, 2006; Evans, 2004). PPARs  $\alpha$ ,  $\gamma$  are already being exploited as pharmacological targets for treatment of obesity and metabolic diseases that ensue, including dyslipidemia, hypertension, atherosclerosis and type 2 diabetes – physiological disorders that besiege an alarming number of adults in the recent years (Evans, 2004). While PPAR $\delta$  has yet to serve the masses as a clinical target, evidence for their potential as drug target for the treatment of metabolic diseases are emerging. Adipose specific over-expression of constitutively active PPAR $\delta$ , via VP16-PPAR $\delta$  construct driven by aP2 promoter, confers protection from diet-induced obesity, steatosis and hyperlipidemia (Wang, 2003). Complimentarily, pharmacological activation of PPAR $\delta$  via its synthetic ligand, GW501516, has been demonstrated to enhance fatty acid oxidation in skeletal muscles and confer protection from high fat diet-induced obesity and insulin resistance (Tanaka, 2003). Molecularly, key genes responsible for fatty acid transport and

subsequent oxidation in myocytes have been shown to be PPAR $\delta$  targets (Ehrenborg, 2009).

The youngest member of the PPAR family, PPAR $\delta$ , is unique in that in addition to its ability to ameliorate signatures of the metabolic syndrome, it is implicated in a variety of physiological processes, including inflammation, neuronal differentiation, mitochondrial respiration, thermogenesis, keratinocyte differentiation, wound healing and skeletal muscle remodeling (Ehrenborg, 2009). In the skeletal muscle, PPAR $\delta$  is expressed at a higher level in the oxidative type I muscles than glycolytic type II muscles (Wang, 2004). Moreover, PPAR $\delta$  activity seems to play an important role in fiber type determination. Skeletal muscle specific over-expression of PPAR $\delta$  induces glycolytic to oxidative fiber type switch (Wang, 2004; Luquet, 2003). Conversely, muscle specific deletion of PPAR $\delta$  reduces the proportion of type I fibers (Schuler, 2006). Additionally, increased expression of its coactivator PGC1 $\alpha$  or the reduction of its corepressor RIP140 increases the proportion of type I fibers in muscle (Lin, 2002; Seth, 2007). Furthermore, molecular characteristics of oxidative fibers, such as higher myoglobin and mitochondrial content, observed in the transgenic models are translatable to a physiological output. Transgenic mice over-expressing constitutively active form of the receptor are able to run 1.75 times longer and twice the distance compared to their wild-type littermates (Wang, 2004).

In this report, we demonstrate that both genetic and pharmacological activation of PPAR $\delta$  promote regeneration after acute thermal injury. PPAR $\delta$  activation during

regeneration expedites resolution of inflammatory response and restoration of contractile proteins. Most interestingly, PPAR $\delta$  activation leads to a transient up-regulation of Notch pathway during early phase of regeneration. Altogether, we offer a novel role of PPAR $\delta$  during adult muscle regeneration and its potential as a therapeutic target to enhance regenerative capacity of skeletal muscle.

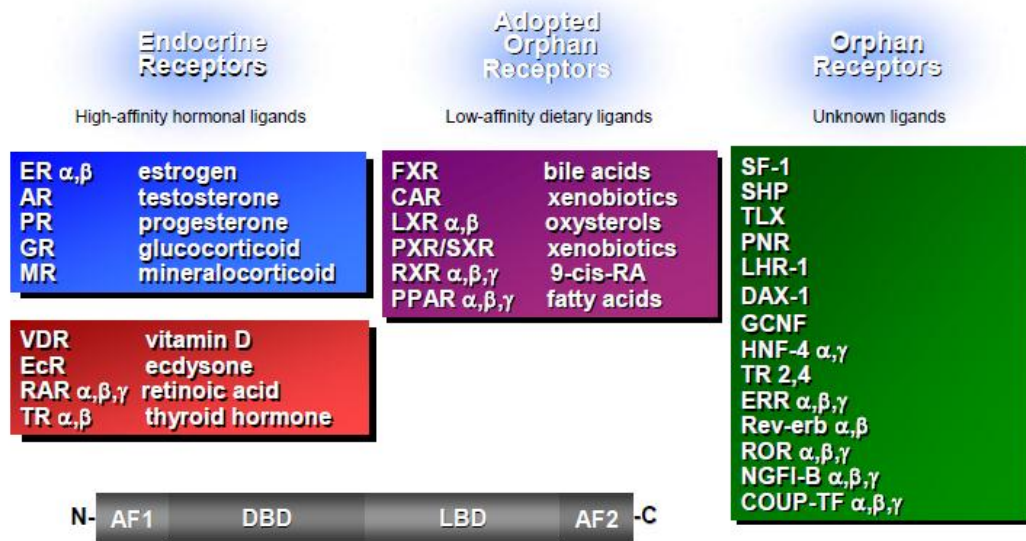


Figure 1.1: Nuclear receptor superfamily. NR family members are classified by their ligand of activation










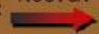
Response Element	Schematic Sequence	NR Mode of Binding	Example
Single Half Site	$(A/T)_n$ 	Monomer	ERRs, COUP-TF, SF1,
Palindromic Repeat:			
Inverted Repeat	 $(N)_n$ 	<ul style="list-style-type: none"> <li>Homodimer AR, ER, GR, MR (3) TR (0)</li> <li>Heterodimer RXR/RAR (0)</li> </ul>	
Everted Repeat	 $(N)_n$ 	<ul style="list-style-type: none"> <li>Homodimer TR (6)</li> <li>Heterodimer RXR/TR (6) RXR/RAR (6)</li> <li>RXR/VDR (9)</li> </ul>	
Direct Repeat	 $(N)_n$ 	<ul style="list-style-type: none"> <li>Homodimer RXR (1) RevErb (2)</li> <li>Heterodimer RAR/RXR (1) RAR/PPAR (1)</li> <li>RXR/RAR (2 or 5) RXR/VDR (3)</li> <li>RXR/TR (4)</li> </ul>	
Archetypal Half-Site:  AGGTCA			

Figure 1.2: Nuclear receptor binding DNA motifs.

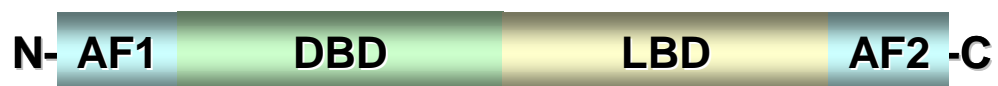


Figure 1.3: Schematic representation of the functional domains of PPARdelta. From the N-terminal: ligand-independent transcription activation (TA) domain, DNA binding domain (DBD), the hinge region (H) and the ligand binding domain (LBD).

## References

- Baar K. Training for endurance and strength: lessons from cell signaling. *Med Sci Sports Exerc.* 2006, 38(11): 1939-1944.
- Barish G.D., Narkar, V.A., and R.M. Evans. PPAR $\delta$ : a dagger in the heart of the metabolic syndrome. *J. Clin. Invest.* 116(3):590-597, 2006.
- Bassel-Duby, R. and E.N. Olson. Signaling pathways in skeletal muscle remodeling. *Annu Rev Biochem.* 2006, 75:19-37.
- Beauchamp, J.R., Heslop, L., Yu, D.S., Tajbakhsh, S., Kelly, R.G., Wernig, A., Buckingham, M.E., Partridge, T.A., and P.S. Zammit. Expression of CD34 and Myf5 defines the majority of quiescent adult skeletal muscle satellite cells. *J. Cell Biol.* 2000, 151: 1221-1234.
- Bober, E., Franz, T., Arnold, H.H., Gruss, P., and P. Tremblay. Pax-3 is required for the development of limb muscles: a possible role for the migration of dermomyotomal muscle progenitor cells. *Development.* 1994, 120: 603-612.
- Bookout AL, Jeong Y, Downes M, Yu RT, Evans RM and DJ Mangelsdorf. Anatomical profiling of nuclear receptor expression reveals a hierarchical transcriptional network. *Cell.* 126(4):789-99, 2006.
- Chawla A., Schwarz E.J., Dimaculangan D.D., and M.A. Lazar. Peroxisome proliferator-activated receptor (PPAR)  $\gamma$ : adipose-predominant expression and induction early in adipocyte differentiation. *Endocrinology.* 136 (2): 798-780, 1994.
- Christ, B., and C.P. Ordahl. Early stages of chick somite development. *Anat. Embryol.* 1995, 191: 381-396.
- Collins, C.A., Olsen, I., Zammit, P.S., Helop, L., Petrie, A., Partridge, T.A., and J.E. Morgan. Stem cell function, self-renewal, and behavioral heterogeneity of cells from the adult muscle satellite cell niche. *Cell.* 2005, 112: 289-301.
- Dellavalle, A. Sampaolesi, M., Tonlorenzi, R., Tagliafico, E., Sacchetti, B., Perani, L., Innocenzi, A., Galvez, B.G., Messina, G., Morosetti, R., Li, S., Belicchi, M., Peretti, G., Chamberlain, J.S., Wright, W.E., Torrente, Y., Ferrari, S., Bianco, P., and G. Cossu. Pericytes of human skeletal muscle are myogenic precursors distinct from satellite cells. *Nat Cell Biol.* 9(3):255-67, 2007.
- Dhawan, J., and T.A. Rando. Stem cells in postnatal myogenesis: molecular mechanisms of satellite cell quiescence, activation and replenishment. *Trends Cell Biol.* 2005, 15(12): 666-673.

Darr, K.C. and E. Schultz. Exercise-induced satellite cell activation in growing and mature skeletal muscle. *J. Appl. Physiol.* 1987, 63(5): 1816-1821.

Dowell P, Peterson VJ, Zabriskie TM and M Leid. Ligand-induced peroxisome proliferator-activated receptor alpha conformational change. *J Biol Chem.* 272(3):2013-20, 1997.

Ehrenborg E and A Krook. Regulation of skeletal muscle physiology and metabolism by peroxisome proliferator-activated receptor delta. *Pharmacol Rev.* 61(3): 373-93, 2009.

Evans R.M., Barish, G.D., and Y.-X. Wang. PPARs and the complex journey to obesity. *Nat Med.* 10(4):1-7, 2004.

Fukada, S., Higuchi, S., Segawa, M., Koda, K., Yamamoto, Y., Tsujikawa, K., Kohama, Y., Uezumi, A., Imamura, M., Miyagoe-Suzuki, Y., Takeda, S., and H. Yamamoto. Purification and cell-surface marker characterization of quiescent satellite cells from murine skeletal muscle by a novel monoclonal antibody. *Exp. Cell Res.* 2004, 296(2): 245-255.

Gros, J., Manceau, M., Thome, V., and C. Marcelle. A common somatic origin for embryonic muscle progenitors and satellite cells. *Nature.* 2005, 435(16): 954-958.

Goulding, M.D., Chalepakis, G., Deutsch, U., Erselius, J.R., and P. Gruss. Pax-3, a novel murine DNA binding protein expressed during early neurogenesis. *EMBO J.* 1991, 10: 1135-1147.

Irintchev, A., Zeschnigk, M., Starzinski-Powitz, A., and A. Wernig. Expression pattern of M-cadherin in normal, denervated, and regenerating mouse muscles. *Dev Dyn.* 1994, 199: 326-337.

Issemann, I. and S. Green. Activation of a member of the steroid hormone receptor superfamily by peroxisome proliferators. *Nature.* 1990, 347(6294): 645-650.

Iwata Y, Miyamoto S, Takamura M, Yanagisawa H and A Kasuya. Interaction between peroxisome proliferators-activated receptor gamma and its agonists: docking study of oximes having 5-benzyl-2,4-thiazolidinedione. *J Mol Graph Model.* 19(6): 536-42, 598-600, 2001.

Kliwer, S.A., Umesono, K., Noona, D.J., Heyman, R.A., and R.M. Evans. Convergence of 9-cis retinoic acid and peroxisome proliferator signaling pathways through heterodimer formation of their receptors. *Nature.* 1992, 358(6389): 771-774.

Kliwer S.A., Forman B.M., Blumberg B., Ong E.S., Borgmeyer U., Mangelsdorf D.J., Umesono K., and R.M. Evans. Differential expression and activation of a family of murine peroxisome proliferator-activated receptors. *PNAS*. 91: 7355-59, 1994.

Laudet, V., and H. Gronemeyer. The nuclear receptor fact book. Academic Press. San Diego. 2002.

Lin J, Puigserver P, Donovan J, Tarr P and BM Spiegelman. Peroxisome proliferator-activated receptor gamma coactivator 1beta (PGC-1beta ), a novel PGC-1-related transcription coactivator associated with host cell factor. *J Biol Chem*. 277(3): 1645-8, 2001.

Luquet, S., Lopez-Soriano, J., Holst, D., Fredenrich, A., Melki, J., Rassoulzadegan, M., and P.A. Grimaldi. Peroxisome proliferator-activated receptor  $\delta$  controls muscle development and oxidative capability. *FASEB J*. 2003, 17(15): 2299-2301.

MacDougall, J.D., Gibala, M.J., Tarnopolski, M.A., MacDonald, J.R., Interisano, S.A., and K.E. Yarasheski. The time course for elevated muscle protein synthesis following heavy resistance exercise. *Can J Appl Physiol*. 1995, 20(4): 480-486.

Mansouri, A., Stoykova, A., Torres, M. and P. Gruss. Dysgenesis of cephalic neural crest derivatives in *Pax7*<sup>-/-</sup> mutant mice. *Development*. 1996, 122: 832-838.

Martins, K.J.B., Gordon, T., Pette, D., Dixon, W.T., Foxcroft, G.R., MacLean, I.M., and C.T. Putman. Effect of satellite cell ablation on low-frequency-stimulated fast-to-slow fibre-type transitions in rat skeletal muscle. *J Physiol*. 2006, 572: 281-294.

Mauro A. Satellite cell of skeletal muscle fibers. *J Biophys Biochem Cytol*. 1961, 9: 493-495.

Moss, F.P. and C.P. Leblond. Satellite cell as the source of nuclei in muscle of growing rats. *Anat. Rec*. 1970, 170: 421-436.

Nolte RT, Wisely GB, Westin S, Cobb JE, Lambert MH, Kurokawa R, Rosenfeld MG, Willson TM, Glass CK and MV Milburn. Ligand binding and co-activator assembly of the peroxisome proliferators-activated receptor-gamma. *Nature*. 395(6698):137-43, 1998.

Peault, B., Rudnicki, M., Torrente, Y., Cossu, G., Tremblay, J.P., Partridge, T., Gussoni, E., Kunkel, L.M., and J. Huard. Stem and progenitor cells in skeletal muscle development, maintenance and therapy. *Mol Ther*. 2007, 15(5): 867-877.

Relaix, F., Rocancourt, D., Mansouri, A., and M. Buckingham. Divergent functions of murine Pax3 and Pax7 in limb muscle development. *Genes & Dev.* 2004, 18: 1088-1105.

Relaix, F., Rocancourt, D., Mandouri, A., and M.E. Buckingham. A Pax3/Pax7-dependent population of skeletal muscle progenitor cells. *Nature.* 2005, 435: 948-952.

Schienda, J., Engleka, K.A., Jun, S., Hansen, M.S., Epstein, J.A., Tabin, C.J., Kunkel, L.M., and G. Kardon. Somitic origin of limb muscle satellite and side population cells. *PNAS.* 2005, 103: 945-950.

Schuler M, Ali F, Chambon C, Duteil D, Bornert JM, Tardivel A, Desvergne B, Wahli W, Chambon P and D Metzger. PGC1alpha expression is controlled in skeletal muscles by PPARbeta, whose ablation results in fiber-type switching, obesity, and type 2 diabetes. *Cell Metab.* 4(5): 407-14, 2006.

Schulman IG, Shao G and RA Heyman. Transactivation by retinoid X receptor-peroxisome proliferators-activated receptor gamma (PPARgamma) heterodimers: intermolecular synergy requires only the PPARgamma hormone-dependent activation function. *Mol Cell Biol.* 18(6): 3483-94, 1998.

Schultz, E., Gibson, M.C., and T. Champion. Satellite cells are mitotically quiescent in mature mouse muscle: an EM and radioautographic study. *J Exp Zool.* 1978, 206(3):451-6.

E. Schultz. Satellite cell proliferative compartments in growing skeletal muscles. *Dev Biol.* 1996, 175: 84-94.

Seale, P., Sabourin, L.A., Girgis-Gabardo, A., Mansouri, A., Gruss, P., and M.A. Rudnicki. Pax7 is required for the specification of myogenic satellite cells. *Cell.* 2000, 102: 777-786.

Seth A, Steel JH, Nichol D, Pocock V, Kumaran MK, Fritah A, Mobberley M, Ryder TA, Rowleron A, Scott J, Poutanen M, White R and M Parker. The transcriptional corepressor RIP140 regulates oxidative metabolism in skeletal muscle. *Cell Metab.* 6(3): 236-45, 2007.

Sherwood, R.I., Christensen, J.L., Conboy, I.M., Conboy, M.J., Rando, T.A., Weissman, I.L., and A.J. Wagers. Isolation of adult mouse myogenic progenitors: functional heterogeneity of cells within and engrafting skeletal muscle. *Cell.* 2004, 119(4): 543-554.

Shi, X., and D.J. Garry. Muscle stem cells in development, regeneration, and disease. *Genes & Dev.* 2006, 20: 1692-1708.

Sinanan, A.C.M., Buxton, P.G., and M.P. Lewis. Muscling in on stem cells. *Biol. Cell.* 2006, 98: 203-214.

Snow, M.H. An autoradiographic study of satellite cell differentiation into regenerating myotubes following transplantation of muscles in young rats. *Cell Tissue Res.* 1978, 186(3):535-40.

Tanaka, T., Yamamoto, J., Iwasaki, S., Asaba, H., Hamura, H., Ikeda, Y., Watanabe, M., Magoori, K., Ioka, R.X., Tachibana, K., Watanabe, Y., Uchiyama, Y., Sumi, K., Iguchi, H., Ito, S., Doi, T., Hamakubo, T., Naito, M., Auwerx, J., Yanagisawa, M., Kodama, T., and J. Sakai. Activation of peroxisome proliferator-activated receptor  $\delta$  induces fatty acid  $\beta$ -oxidation in skeletal muscle and attenuates metabolic syndrome. *Proc Natl Acad Sci USA.* 100(26):15924-15929, 2003.

Tomaru T, Satoh T, Yoshino S, Ishizuka T, Hashimoto K, Monden T, Yamada M and M Mori. Isolation and characterization of a transcriptional cofactor and its novel isoform that bind the deoxyribonucleic acid-binding domain of peroxisome proliferators-activated receptor-gamma. *Endocrinology.* 147(1):377-88, 2006.

Umnova, M.M., and T.P. Seene. The effect of increased functional load on the activation of satellite cells in the skeletal muscle of adult rats. *Int J Sports Med.* 1991, 12(5):501-504.

Vierck, J., O'Reilly, B., Hossner, K., Antonio, J., Byrne, K., Bucci, L., and M. Dodson. Satellite cell regulation following myotrauma caused by resistance exercise. *Cell Bio Int.* 2000, 24: 263-272.

Wagers, A.J. and I.M. Conboy, Cellular and molecular signatures of muscle regeneration: current concepts and controversies in adult myogenesis. *Cell.* 122: 659–667, 2005.

Wang Y.X., Lee C.H. Tjep S., Yu R.T., Ham Y., Kang H., and R.M. Evans. Peroxisome proliferator-activated receptor  $\delta$  activates fat metabolism to prevent obesity. *Cell*, 113: 159-170, 2003.

Wang, Y.-X., Zhang, C.-L., Yu, R.T., Cho, H.K., Nelson, M.C., Bayuga-Ocampo, C.R., Ham, J, Kang, H., and R.M. Evans. Regulation of muscle fiber type and running endurance by PPAR $\delta$ . *PLoS Biol.* 2(10): e294, 2004.

Zierath JR and JA Hawley. Skeletal muscle fiber type: influence on contractile and metabolic properties. *PLoS Biol.* 2(10):e348, 2004.

## **Chapter 2:**

**Effects of muscle specific activation of  
PPARdelta during skeletal muscle regeneration  
after acute injury.**



## **Abstract**

Muscle specific over-expression of constitutively active PPAR $\delta$  induces fiber type remodeling and concomitant changes in metabolic and functional capacity of the muscle (Wang, 2004). We sought to test whether PPAR $\delta$  mediated muscle remodeling also alters the regenerative capacity of the muscle. We employed the transgenic mouse model bearing skeletal muscle specific expression of constitutively active PPAR $\delta$  (VP16-PPAR $\delta$ ) to examine the regenerative response to acute thermal injury. PPAR $\delta$  activation promoted restoration of fiber integrity and nascent fiber formation. Furthermore, PPAR $\delta$  activation potentiated resolution of inflammatory response and induction of myogenic markers. Additionally, we observed a 40-60% higher number of proliferating cells after the injury, which coincided with elevated expression of Notch signaling pathway components during the early phase of the regenerative process. Finally, VP16-PPAR $\delta$  animals exhibited ~6 fold increase in the number of resident satellite cells. Collectively, we demonstrate that muscle specific activation of PPAR $\delta$  is sufficient to confer regenerative advantage after an acute muscle injury.

## Introduction

Skeletal muscle is a mechanically and energetically active organ, supporting vital functions such as breathing, locomotion, and glucose and lipid metabolism. Therefore, maintaining proper function is critical for the success of an individual. Inevitably, skeletal muscle suffers damage through a variety of stimuli: acute injury by physical, mechanical or chemical insults, chronic state of pathology and simply, aging. While skeletal muscle does not undergo constant turn-over under normal conditions, upon receipt of damage, it is capable of executing robust regenerative response through mobilization of its resident progenitor cells (Moss, 1970; Schultz, 1978; Snow, 1978).

Upon injury, skeletal muscle promptly responds to damage in three distinct but overlapping phases: degeneration, regeneration and finally remodeling phase (Charge, 2004). Immediately following the injury, inflammatory cells such as neutrophils and macrophages are recruited to the injury site via release of cytokines, such as HGF, IL-6, -15 and LIF, from the compromised myofibers (Tidball, 200; McLennan, 1996; Pimorady-Esfahani, 1997; Vierck, 2000). Myeloid cells promote tissue necrosis by cell lysis and debris clearance by phagocytosis, but also actively facilitate the regenerative process (Arnold, 2007). The regenerative process is characterized by mobilization of satellite cells. Through various *in vivo* and *in vitro* studies, monocytes and macrophages have been shown to interact - via chemotaxis – with satellite cells to promote proliferation and thus myogenesis (Charge, 2004; Robertson, 1993; Cantini, 1995a; Chazaud, 2003; Tidball, 2007). In culture, monocytes promote autocrine secretion of IL-6 by satellite cells, which in turn stimulate their proliferation (Cantini, 1995b). Satellite cells comprise less than 5% of total nuclei on an adult myofiber,

nevertheless, based on their proliferation kinetics and capacity, they are sufficient to regenerate an entire muscle (Schmalbruch, 1977; Kelly, 1978; Gibson, 1982; Bischoff, 1994; Zammit, 2002). Additionally, proliferation and differentiation of the satellite cells are tightly controlled by the signaling tag team of Notch and Wnt pathways during the regeneration phase (Brack, 2008). Temporal and spatial regulation Notch signaling is necessary for expansion and replenishment of the satellite cell pool (Conboy, 2002). Forced activation of Notch-1 rejuvenates muscle regeneration in aged mice while inhibition interferes with muscle regeneration on young mice (Conboy, 2003). Lastly, remodeling phase concludes the regeneration process by reassembling contractile proteins to restore muscle function.

Inherently, slow and fast muscles can respond differently to various conditions leading to muscle damage. In age-induced muscle loss, preferential atrophy occurs in type II fibers, along with preferential loss of satellite cells from type II fibers (Larsson, 1978; Lexell, 1988; Lexell and Downham, 1992; Verdijk, 2007). In ischemia-reperfusion injury model, predominantly slow-fiber consisting muscle, i.e. soleus, suffers less damage than predominantly fast-fiber consisting muscles, i.e. EDL, plantaris, TA (Walters, 2008; Gardner, 1984; Jennische, 1985; Woitaske, 1998; Chan, 2004). Additionally, soleus muscles show accelerated structural and functional recovery after ischemic injury, albeit, soleus muscle suffer inefficient and aberrant regeneration after injuries causing nerve damage (Woitaske, 1998; Chan, 2004; Carvalho, 1995; Kalhovde, 2005; Zimowska, 2001).

Freeze burn injury has been widely used to simulate acute injury to the muscle (Schiaffino and Partridge, 2008). It elicits standard course of regenerative response from the

muscle, including satellite cell activation. However, it is not severe enough to completely incapacitate the animal. The damaged fibers regain their cross sectional area by 21 days after the injury. Additionally, since the injury is directly applied to the surface of the muscle, it is highly localized and reproducible.

We and others have shown that the activation of peroxisome proliferators activated receptor  $\delta$  (PPAR $\delta$ ) induces fiber type switch toward oxidative phenotype, altering both metabolic and functional output of the muscle (Wang, 2003, Luquet, 2003). Recently, endurance exercise alone has been shown to improve ageing induced decrease in satellite cell number and their myogenic capacity (Shefer, 2010). Therefore, we sought to determine if transcriptionally modulated endurance phenotype by PPAR $\delta$  activation confers regenerative advantage after acute muscle injury.

In this report, we demonstrate that the genetic activation of PPAR $\delta$  promote muscle regeneration after acute thermal injury. Muscle specific PPAR $\delta$  activation during regeneration expedites resolution of inflammatory response and restoration of contractile proteins. Most interestingly, PPAR $\delta$  activation leads to a transient up-regulation of Notch pathway during early phase of regeneration. Altogether, we offer a novel role of PPAR $\delta$  during adult muscle regeneration and its potential as a therapeutic target to enhance regenerative capacity of skeletal muscle.

## Materials and Methods

### Animals

VP16-PPAR $\delta$  mice (Wang, 2004) were bred to CB6F1 strain (Jackson Laboratories) and used as heterozygotes in experiments. The wildtype littermates served as controls. All experiments were performed when animals were 8 weeks of age, unless otherwise noted. Skeletal muscle specific PPAR $\delta$  knock-out mice were generated by crossing animals carrying *loxP* sites around exon 4 of PPAR $\delta$  gene (Barak, 2002) and MCK-Cre, which restricts expression of Cre recombinase to mature muscles (Bruning, 1998). For experiments, animals that are homozygous for *loxP* PPAR $\delta$  allele with or without the concurrent expression of Cre recombinase were used. Nestin-GFP mice (Mignone, 2004) were kindly provided by Dr. Fred Gage at the Salk Institute for Biological Studies. They were bred with VP16-PPAR $\delta$  animals to generate double transgenic animals. Single transgenic animals positive for GFP expression were used as controls.

### Fiber typing gel

The proportion of each fiber type in a muscle group was calculated by separating myosin heavy chain isoforms on PAGE according to a published protocol with a few modifications (Mizunoya, 2008). Muscle tissues were harvested and roughly minced by a razor blade. Minced tissue was placed in Homogenization Buffer (10% SDS, 40mM DTT, 5mM EDTA, 0.1M Tris-HCl, pH 8.0, and protease inhibitor cocktail (Roche)) and homogenized with Dremel hand-held homogenizer at the setting of “15” for 10 seconds or until no residual tissue pieces were visible. Samples were

boiled at 100°C for 5 minutes, then diluted (Soleus: 1/400; TA: 1/20,000) with Homogenization Buffer and mixed with 2X Loading Buffer (1%  $\beta$ -Mercaptoethanol, 4% SDS, 0.16M Tris-HCl, pH 6.8, 43% glycerol and 0.2% Bromophenol Blue). Prepare 0.75mm thick gels (Separating gel: 8% x/v Acrylamide-Bis (99:1), 0.2M Tris-HCl, pH 8.8, 0.1M Glycine, 0.4% w/v SDS, 0.1% w/v APS, 35% glycerol, 0.05% TEMED; Stacking gel: 4% w/v Acrylamide-Bis (50:1), 70mM Tris-HCl, pH 6.7, 4mM EDTA, 0.4% w/v SDS, 0.1% APS, 30% glycerol, 0.05% TEMED) and load 10ul per well per sample and run at constant 40mA through the stacking gel and constant 140V thereafter for 22 hours in the cold room. MHC isoforms were visualized using SilverSNAP Stain Kit II (Pierce) by following the kit's instructions. Gels were air dried for several days in between cellophane sheets.

### **Freeze burn injury**

Tibialis anterior muscles were injured according to previously published methods with a few modifications (Brack, 2007). The animals were anesthetized by Isofurane inhalation during the procedure. The skin was shaved over the TA muscles on both legs and the area was cleaned with 100% isopropynol. A small incision was made on the skin to expose the TA muscle. On the control leg, the incision was mended without further treatment. On the experimental leg, a stainless-steel 1g weight equilibrated to the temperature of dry ice was placed directly on the exposed TA for 10 seconds. Following the thermal injury, incision was closed using VetBond. All injury procedures were performed on the left leg, and the right leg was used as

control. The injured portion of the muscle was carefully removed for gene expression analyses.

### **Histology**

Animals were perfused with 15 ml of ice-cold PBS followed immediately by 20 ml of 10% saline buffered formalin (Fisher). Tibialis anterior muscles were excised and immersed in 4% paraformaldehyde (EMB) for at least 48 hours at 4°C. Tissues were washed thrice in PBS for 10 minutes each, at room temperature with gentle rocking. Tissues were sequentially dehydrated in the following order: 25%, 50%, 75%, 95% and 100% ethanol, 20 minutes each with two changes of solution at each concentration for the total of 40 minutes in each concentration. Finally, tissues were cleared in three changes of xylene at 10 minutes each. Xylene was replaced by paraffin for a few hours at 60°C then changed to fresh paraffin to let it permeate through the tissues over night. Tissues were then embedded in plastic molds.

Paraffin embedded tissue blocks were sectioned at 7 um thick on Leica Jung 2500 Microtome. 3-5 sections were acquired per step, 2 slides per step and each step was separated by 200 um. One slide from each step was H&E stained, on average 10 slides per animal, where “step” with the largest injury area was deemed as the center of the injury and used for analyses. For H&E staining, sections were de-paraffinized and rehydrated by submerging in the following: 3x xylene, 3 minutes each; 2x 100%, 90%, 75% ethanol for 2 minutes each; 50% ethanol for 2 minutes and ddH<sub>2</sub>O for 2 minutes. Slides were then stained in 50/50 Gill’s No2 Hematoxylin/H<sub>2</sub>O mixture. After 5 minutes, slides were placed under running tap water for 5 minutes and

dehydrated in the following sequence: 50%, 75% and 95% ethanol for 2 minutes each. Slides were counter stained in 1% eosin (1% eosin Y in 95% ethanol with 500ul glacial acetic acid) solution for 2 minutes. Slides then underwent two changes of 100% EtOH for 2 minutes each. Finally, they were cleared in three changes of xylene at 5 minutes each. Slides were dried under the fume hood and mounted with Entellen mounting media.

Three random non-overlapping fields were photographed for analysis. Regenerating fiber number was measured by counting the number of discernible muscle fibers with centralized myonuclei (Ge, 2009). Regenerating fiber cross sectional area (CSA) was measured using Image J software.

### **BrdU staining**

50mg/kg body weight of BrdU (Sigma) was injected intraperitoneally as solution of 10mg/ml BrdU in saline, either at 12, 24 or 48 hours after the freeze burn injury. TA muscles were harvested at 7 days after injury and processed for paraffin sections as described above. BrdU incorporation was visualized using the BrdU Labeling and Detection Kit I (Roche) and the slides were mounted with Vectashield with DAPI (Vector Labs).

### **Evans Blue dye staining**

Injured animals were injected with Evans Blue dye according published protocol (Hamer et al., 2002). Sterile 1% w/v Evans Blue dye in PBS was intraperitoneally injected at 1% volume relative to the animal's body mass. 7 hours after the injection, injured TA muscles were harvested. TA muscles were placed on a



mound formed by mixing gum tragacanth with O.C.T. compound and snap-frozen by isopentane quenching in liquid nitrogen. The frozen tissues were stored at  $-80^{\circ}\text{C}$ .

Frozen sections were cut in  $10\mu\text{m}$  thickness and dried at room temperature for at least 1 hour. Sections were then fixed in ice-cold acetone for 2 minutes, air dried and quickly dipped in xylene. Dehydrated sections were mounted under coverslips with DPX. Sections were analyzed with the Rhodamine channel setting of the Leica fluorescent microscope. Amount of staining was measured by ImageJ software.

### **Isolation and culture of satellite cells**

Satellite cells were harvested from TA, gastrocnemius and soleus of 8 weeks old animals according to published protocols with some modifications (Day, 2007). Muscles were removed and washed briefly in DMEM on ice. They were then minced to fine slurry with razor blade on 60mm culture dish over ice. Minced muscles were transferred to one well of a 6-well plate containing 5 ml of 450KPU/ml pronase in DMEM with 10% FBS. The tissues were digested at  $37^{\circ}\text{C}/5\% \text{CO}_2$  for 60 minutes. Tissues were vigorously triturated 20 times through 10ml serological pipet. Digested tissues were filtered through 40 micron cell strainer and washed with equal volume of DMEM supplemented with 20% horse serum. Cells were spun down at 1000rpm and resuspended in either sorting buffer (DMEM with 10% FBS) or growth media (DMEM with 20% FBS, 10% HS, 1% CEE and 100U penicillin and 100ug/ml streptomycin). Cells were plated on culture dishes coated with 10ug/ml of laminin (Blanco-Bose, 2001). During subsequent splittings, in order to eliminate contaminating fibroblasts and enrich for the myoblasts, cells were pre-plated on tissue

culture plates for 15-60 minutes. The medium containing the cells that did not adhere during pre-plating were then plated and maintained on fresh laminin coated plates.

### **RT-QPCR**

Whole or partial tissues were homogenized by Polytron probe homogenizer in Trizol reagent (Invitrogen). 3ml of Trizol was used for up to 50mg of tissue and the homogenizer was set at level 5 and applied to the samples for 7 seconds. Total RNA was extracted from the homogenates according to the manufacturer's protocol with a few alterations: after the phases were separated, aqueous phase containing RNA was loaded onto the RNeasy Mini kit (Qiagen) to clean and isolate RNA according to the kit instructions. RNA concentrations were measured spectrophotometrically on NanoDrop 8000 (Thermo Scientific). 1 $\mu$ g of total RNA was reverse transcribed (RT) using Superscript II (Invitrogen) or iScript Reverse Transcription Supermix (BioRad) according to the respective manufacturer's instructions. cDNAs were diluted 1/40 with ddH<sub>2</sub>O and used as templates in RT-QPCR reactions with SYBRGreenER qPCR SuperMix detection system. qPCR reactions were performed on 7900HT Fast Real-Time PCR system (Applied Biosystems). Data were processed and analyzed using the SDS Software v2.4 (Applied Biosystems).

After isolation, satellite cells were FACS sorted for their GFP expression on BD FACSAria flow cytometer. Sorted cells were processed as above to isolate RNA, except RNeasy Micro kit (Qiagen) was used to efficiently procure small amount of RNA. Isolated RNA was amplified using the WT Ovation RNA Amplification System (NuGEN) according to the manufacturer's protocol.

## Primers

Q-PCR primers were constructed by “Pick Primers” function on NCBI website for each gene. PPAR $\delta$  F:GCCTCGGGCTTCCACTAC, R: AGATCCGATCGCACT TCTCA; VP16 F: CGCTAGACGATTTTCGATCTGGAC, R: CGGTAAACATCTGCTCAAACCTCG; PDK4: 3’GCCATTATAAAGAAAGCAACTAAGCA, 5’ CCAGAGACGCGTATTTCTACCA; CPT1 $\beta$ : 3’GGGTCCCAAAGTGGCCA, 5’ CATGGGACTGGTTCGATTGC; catalase F:AGCGACCAGATGAAGCAGTG, R: TCCGCTCTCTGTCAAAGTGTG ; MCP1 F: GGCTCAGCCAGATGCAGTTAA, R: CCTACTCAT TGGGATCATCTTGCT; MyoD F: GCCGCTGAGCAAAGTGAATG, R: CAGCGTCCAGGTGCGTAGAAG; MYH8 F: CGTACGGTGTATCATTCCCAATG, R:TGTGTCAGGACCAGTTCGT; Notch1: 3’ GAG CCCTCGTTGCAGGGGTT, 5’ CTGCGAATGTCCGCATGGGC; Hey1: 3’ GCGAAGGGCTGGGGGTAGTC, 5’ CTTTCGGCATGAAGCGGCCC; HES1 F: GGAGAAGAGGCGAAGGGCAAGA, R: TGCAGGTTCCGGAGGTGCTT; HEY1 F: CTTTCGGCATGAAGCGGCCC, R: GCGAAGGGCTGGGGG TAGTC; Pax7 F: CTCAGTGAGTTCGATTAGCCG, R: AGACGGTTCCTTTGT CGC; Tuj1 F: CCAGACCGAACACTGTCCA, R: CCCAGCGGCAACTATGTAGG

## Myofiber isolation

Individual myofibers were isolated according to published protocol with slight modifications (Rosenblatt, 1995). Gastrocnemius muscles were dissected and placed in glass scintillation vials or 5ml glass test tubes. Muscles were digested in 0.2% (w/v) collagenase I in DMEM for 1 hour at 35 °C with gentle shaking in a water bath

(Sigma). Loosely liberated myofibers were mechanically individualized by repeated trituration using wide-mouthed, fire-polished-tip Pasteur pipets in PBS supplemented with 10% FBS. Isolated myofibers were washed thrice with PBS with 10% FBS and immediately mounted on glass slide with Vectashield or fixed in 4% paraformaldehyde.

### **Cryosection and immunofluorescence staining**

Frozen muscle tissues were transversely sectioned at 7-10  $\mu\text{m}$  thickness on Leica CM1850 cryostat. Sections were dried on slides at room temperature for at least 1 hour prior to storage at  $-80\text{ }^{\circ}\text{C}$ .

For IF, slides were allowed to equilibrate to room temperature for at 15 minutes. If the sections were mounted in O.C.T., slides were washed twice in PBS for 3 minutes each to remove the mounting media. Sections were then fixed in pre-cooled 50/50 acetone/methanol mixture for 20 minutes at  $-20\text{ }^{\circ}\text{C}$ . Slides were washed thrice in PBS at room temperature for 2 minutes each to remove the fixative. Tissues were blocked in 10% goat serum (GS) for 1 hour at room temperature. Afterwards, tissues were incubated in primary antibody over night at  $4\text{ }^{\circ}\text{C}$  in humidified chamber. Excess antibody and loosely bound non-specific interactions were removed by three washes in 0.01% Tween-20/PBS at 5 minutes each. Sections were then incubated in appropriate secondary antibody at room temperature for 30 minutes. Slides were washed thrice in 0.01% Tween-20/PBS at 5 minutes each and mounted under coverslips with Vectashield with DAPI. Where appropriate, M.O.M. Fluorescein staining kit (Vector

Labs) was used according to the manufacturer's instructions. Antibody dilutions:

Pax7 – 1:2500, CD31 – 1:400.

## Results

### *Muscle specific activation of PPAR $\delta$ confers regenerative advantage*

We tested the regenerative capacity of VP16-PPAR $\delta$  using the freeze burn injury (Conboy, 2003). Majority of the metabolic genes are down regulated in response to freeze burn injury (Summan, 2003). Curiously, PPAR $\delta$  expression was induced over 2 fold at 2 days after the injury, eventually returning to the basal level by day 7 (Figure 2.1A). Injury dependent up-regulation of PPAR $\delta$  suggests a positive role for PPAR $\delta$  during the early part of the regenerative process. First, we grossly assessed the fiber integrity 5 days after thermal injury using Evans Blue uptake (Figure 2.1B). Evans Blue dye penetration was used as a marker of myofiber damage to assess regeneration (Hamer, 2002). Injected dye permeates into the syncytia of non-intact fibers, while being excluded from the intact fibers. By comparing the proportion of stained fibers within cross sections of the injured muscle, we determined the permeability, thus degree of damage. At 5 days after the injury, VP16-PPAR $\delta$  animals show significant improvement over the WT animals. While WT animals show staining of 14% of the total CSA, i.e. the proportion of non-intact fiber area, only 5% of VP16-PPAR $\delta$  muscle was stained by the dye ( $p=0.001$ ) (Figure 2.1C). At 12 and 36 hours after the thermal injury, both WT and VP16-PPAR $\delta$  animals showed similar proportions of stained area (50.6% and 47.4% ( $p=0.67$ ), and 38.5% and 43.3% ( $p=0.228$ ), respectively) (Figure 2.1D). This suggests that both WT and VP16-PPAR $\delta$  animals initially sustain similar degree of damage due to the thermal injury.

The reduction in the stained area suggests that the muscle specific PPAR $\delta$  activation is sufficient to facilitate accelerated progression through the regenerative program.

We then examined other markers of regeneration, namely the morphological hallmarks of regenerating fibers. H&E stained transverse sections through the injured area were examined at 3, 5 and 7 days post injury. At 3 days after the injury, both wildtype and VP16-PPAR $\delta$  mice show similar degrees of destruction – necrosing fibers surrounded by infiltrating monocytes (Figure 2.2A). No regenerating fibers, characterized by small, round shape and centralized nuclei, are discernible at this time point in wildtype animals, but a notable few were seen in TG animals (arrows, Figure 2.2A). By day 5 after the injury, obvious differences begin to emerge. In wildtype animals, small regenerating fibers are visible but necrosing fibers and monocytes are still prevalent at the site of the injury (arrowheads, Figure 2.2A). While in VP16-PPAR $\delta$  animals, the injury site seems relatively sound, with prominence of regenerating fibers. By day 7 post injury, the injury site appears similar between the two groups; where both show a field of regenerating fibers with centralized nuclei, most of the infiltrating cells have retreated and damaged fibers appear to have been properly managed. However, quantification of regenerating fiber number and CSA reveals that by 5 days post injury, the regenerative advantage of VP16- PPAR $\delta$  is clearly discernible. Both CSA of the regenerating fibers and the number of regenerating fibers were 43.5% (n=5 or 6; p<0.03) and 33.0% (n=11 or 12; p<0.001), respectively, greater for VP16- PPAR $\delta$  animals (Figures 2.2B&C). At 21 days after the injury, both WT and VP16- PPAR $\delta$  animals have restored their fiber size and

number to that of the uninjured level (Figure 2.2D). These data demonstrate that the muscle specific activation of PPAR $\delta$  sufficiently bestows regenerative advantage over their wildtype counterparts.

*PPAR $\delta$  activation leads to temporal shift, thus increased efficiency, of the regenerative process*

Skeletal muscle regeneration is an intricately orchestrated process involving a variety of cell types. Therefore, we then decided to examine the effects of PPAR $\delta$  activation in the non-myogenic arm of the regenerative process in our injury model. Immune cells, both neutrophils and macrophages, are necessary for the proper progression of regenerative process (Zacks, 1982; Grounds, 1987; Teixeira, 2003; Summan 2006; Contreras-Shannon, 2007; Segawa, 2008). Additionally, various cytokines are necessary to promote chemotaxis of monocytes and also to directly regulate the activities of myogenic cells (Warren, 2004; Yahiaoui, 2008; Chazaud, 2003).

We first identified a global, injury specific gene expression changes in VP16-PPAR $\delta$  animals. Comparing the gene expression profiles of injured to TG to WT, there were total of 3257 genes that changed expression, of those, 1375 of them were down regulated and 1882 were up regulated. Gene ontology classification of up-regulated genes revealed that cellular processes (i.e. organization, localization, signaling), metabolic processes (i.e. fatty acid oxidation) and response to stimuli (i.e. response to stress, defense response) were the top regulated processes by the activation of PPAR $\delta$  at 3 days after the injury (Figure 2.3). Interestingly, genes involved in



myogenesis were robustly up-regulated by PPAR $\delta$  activation (Figure 2.3).

Additionally, genes involved in developmental processes, angiogenesis and anti-apoptotic processes emerged from the analysis (Figure 2.3). Collectively, PPAR $\delta$  activation appears to control network of genes involved directly in myogenesis and also in remodeling and repair process after injury.

In order to validate and temporally expand microarray data, expression of select inflammatory (TNF $\alpha$  and CD68) and myogenic (MyoD) markers were measured by QPCR (Figure 2.4A&B). In short, we observed a temporal shift in the expression patterns of regenerative markers for VP16-PPAR $\delta$  animals compared to their wildtype littermates. Specifically, VP16-PPAR $\delta$  animals showed earlier induction of inflammatory genes whose expressions peaked sooner and were subsequently down regulated earlier than in the wildtype animals. Interestingly, inflammatory markers studied here peaked at similar levels between the two genotypes, which suggests that VP16-PPAR $\delta$  animals do not completely suppress their inflammatory responses. Instead, it appears that VP16-PPAR $\delta$  animals respond and resolve their inflammatory responses more efficiently. Furthermore, VP16-PPAR $\delta$  animals show higher expression of perinatal myosin heavy chain gene, Myh8, a regeneration marker (Figure 2.4C).

#### *PPAR $\delta$ activation positively regulates quiescent satellite cell number*

In order to determine cellular basis for the regenerative advantage conferred by PPAR $\delta$  activation, we sought to quantify satellite cells number in uninjured VP16-

PPAR $\delta$  animals using nestin as a marker (Day, 2007). We thus created nestin-GFP;VP16-PPAR $\delta$  double transgenic animals to genetically mark quiescent satellite cells in vivo (Mignone, 2004). Gastrocnemius muscles were enzymatically digested to liberate individual fibers, then mounted for quantification of the number of GFP+ SCs. While double transgenic animals averaged 1.01 SCs per mm of fiber length, GFP+ animals only had 0.15 SCs per mm, a 6.48 fold higher SC content on VP16- PPAR $\delta$  muscle fiber (Figure 2.5A&B). In order to confirm functionality of the increased satellite cell number, we measured satellite cell activity as myoblast proliferation elicited by the freeze burn injury in vivo. After the freeze burn injury, BrdU was intraperitoneally injected at 12 hrs, 24 hrs and 2 days after the injury and the muscles were harvested 7 days after the injury to calculate the ratio of BrdU+ to total nuclei. TG animals showed 40-60% increase in the number of BrdU+ proliferating cells at all three injection times (Figure 2.6A). Notch signaling is activated and necessary during the early phase of regeneration to support myoblast proliferation (Brack, 2008). Most interestingly, gene expression analysis revealed injury induced Notch1 and its ligand, Delta1, up-regulation is transiently amplified in TG animals (Fig 2.6B&E). Concomitantly, Notch1 target gene, Hey1 and Hes1, is also induced at a higher level, demonstrating that PPAR $\delta$  activation during injury enhances Notch signaling to promote myoblast proliferation (Figure 2.6C&D).

*Skeletal muscle remodeling conferred by PPAR $\delta$  activation exerts satellite cell non-autonomous effects to facilitate regenerative advantage.*

The use of human skeletal  $\alpha$ -actin promoter limits, in theory, the expression of the transgene to the myonuclei in mature myofibers. We confirmed the expression of

the transgene to be absent in freshly isolated quiescent satellite cells (Figure 2.7A&B). This suggests that the regenerative advantage conferred by PPAR $\delta$  activation is not satellite cell autonomous. We sought to determine an adaptive response bestowed by PPAR $\delta$  activation in the muscle which may be contributing to the observed beneficial effects on regeneration. Increased vasculature is one of the hallmarks of oxidative myofibers, which is known to facilitate introduction of immune cells and also supports increased number of satellite cells. Immunostaining transverse sections of uninjured TA from WT and TG animals revealed 36% increase in the number of CD31+ capillaries per field by PPAR $\delta$  activation (Figure 2.8A&B). Furthermore, microarray analysis shows significant increases in angiogenic genes, VEGFa, VEGFb and FGF1, by PPAR $\delta$  activation (Figure 2.8C). Microarray data for the expression of VEGFa was confirmed by QPCR (Figure 2.8D). While it is possible that there is some signal being transmitted from the myofiber to the satellite cells and other types of cells involved in regenerative process to accelerate the process, increased vascularity could at least contribute to this phenomenon.

## Discussion

We herein report that PPAR $\delta$  activation expedites skeletal muscle regeneration following an acute thermal injury. VP16- PPAR $\delta$  transgenic animals showed increased satellite cell proliferation at the early phase of the regenerative process, which subsequently translated into increased CSA and the number of nascent regenerating fibers. Most interestingly, we have learned that the PPAR $\delta$  activation augments transient Notch signaling during the early phase of regeneration, which maybe driving the increased proliferation in these animals after the injury. Additionally, muscle specific over expression of PPAR $\delta$  seems to increase the resident satellite cell pool. Increased satellite cell population on a muscle fiber seems to, at least in part, contribute to the accelerated resolution of the injury. These findings unveil a novel role for PPAR $\delta$  in the maintenance of skeletal muscle; as a potential therapeutic target for accelerated restoration of muscle mass after an acute injury and other atrophic conditions.

Notably, PPAR $\delta$  activation seems to promote rapid emergence of nascent fibers after the injury. There being no evidence of hyperplasia at 21 days after the injury when the regenerative process is essentially complete, we conclude that the additional nascent fibers efficiently fuse with each other to restore mature fibers (Karpati, 2008). While IGF-1 and myostatin seem to rely on fiber hypertrophy to augment regenerative progress, PPAR $\delta$  seems to employ a unique way to promote regeneration (Menetrey, 2000; Wagner, 2002; Bogdanovich, 2002). Underlying this difference may be the increased number of quiescent satellite cells. Higher number of

progenitor cells leads to the increase in post injury proliferating cells and consequent increase in the number of nascent fibers. While various growth factors and chemokines, including IGF-1 and myostatin, have been shown to enhance proliferation of satellite cells and promote regeneration, it is unclear whether any of them positively regulate the number of quiescent satellite cells (Husmann, 1996; McCroskery, 2003; Musaro, 2001; Amthor, 2009). Our findings strongly suggest a novel role of PPAR $\delta$  as a positive regulator of satellite cell pool. Notably, the direct role of PPAR $\delta$  in satellite cell homeostasis was recently reported using Myf5-Cre conditional knockout model (Angione, 2011). Interestingly, since we did not observe constant cell proliferation under normal condition, PPAR $\delta$  mediated satellite cell expansion is transient and tightly regulated, most likely elicited by external stimuli, such as signals for postnatal growth and injury. Moreover, in VP16-PPAR $\delta$  model, transgene is over-expressed only in the mature fiber, thereby suggesting indirect effects on satellite cell homeostasis through soluble factors or solicitation of other changes in the muscle. Nevertheless, in an adult muscle, satellite cell number is finite, diminishing detrimentally in disease state and aging. It is of great therapeutic benefit if PPAR $\delta$  activation can bestow infinite abundance of satellite cell population throughout the life of an organism.

Chapter 2, in part, is currently being prepared for submission for publication. Embler, EK; Atkins, A; Downes, M; Evans RM. The dissertation author was the primary investigator and author of this material.

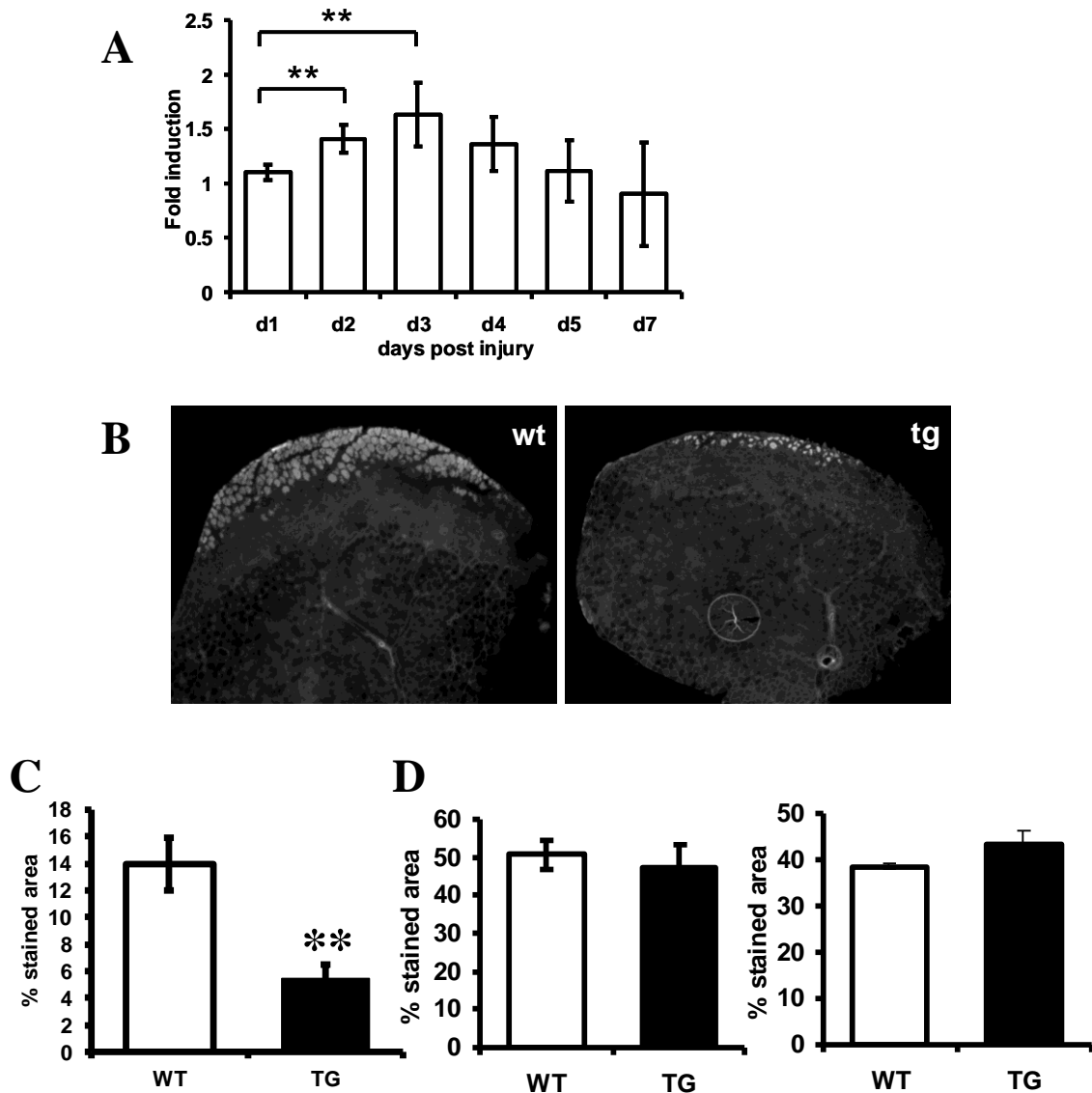


Figure 2.1: VP16-PPAR $\delta$  animals show increased efficiency in restoration of fiber integrity after injury. A) thermal injury was administered to the TA of 8 week-old wildtype animals and the injured portion was removed for expression of PPAR $\delta$  by QPCR. B) 8 week-old VP16-PPAR $\delta$  animals and their littermate controls were injured then allowed to recover for 5 days (n=8 for WT; n=5 for TG). Evans Blue dye was injected intraperitoneally to detect fiber permeability. C) Proportions of damaged area were calculated as percentage of stained area over total cross sectional area of TA. D) 8 week-old VP16-PPAR $\delta$  animals were injured as above, and fiber integrity was measured at either 12 or 36 hours post injury by Evans Blue dye injection (n=3, each genotype).

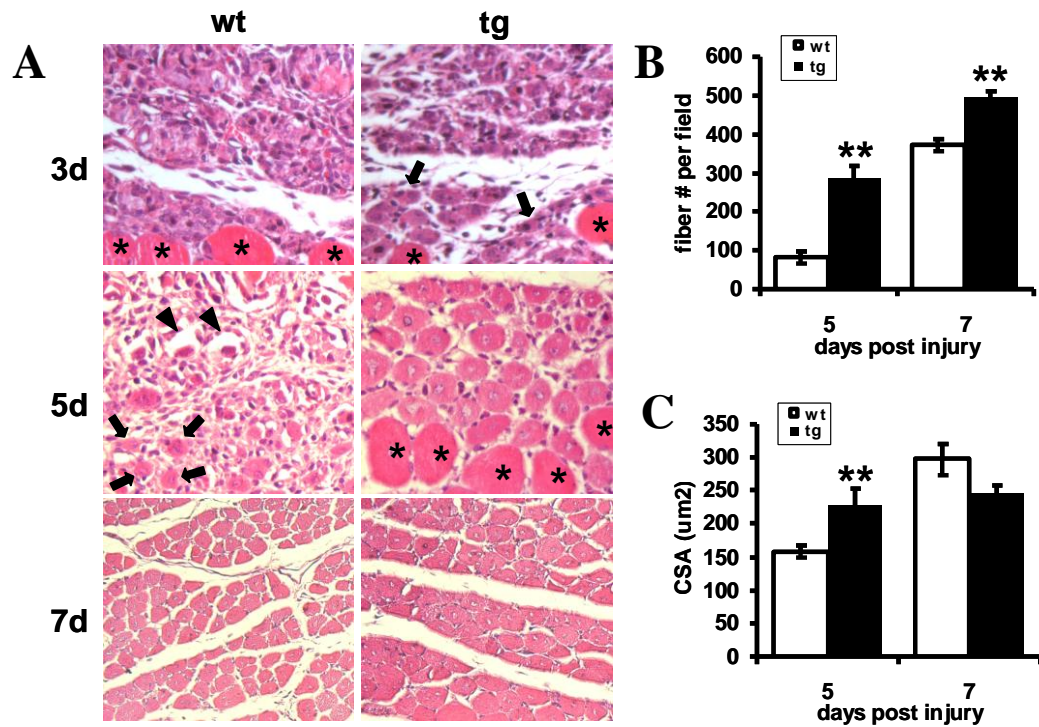


Figure 2.2: Skeletal muscle specific activation of PPARdelta expedites regenerative process after acute injury. A) H&E stained transverse sections of injured TA from wild-type (WT) and VP16- PPAR $\delta$  (TG) animals were morphometrically analyzed (n=6 to 12 each genotype). TAs were harvested at 3, 5 and 7 days after injury. Regenerating fibers with centralized nuclei are marked by arrows. Arrowheads denote hollowed remains of basal lamina. Uninjured fibers are marked by asterisks. B) Quantification of the number of regenerating fibers per field. C) CSA of regenerating fibers measured by Image J.

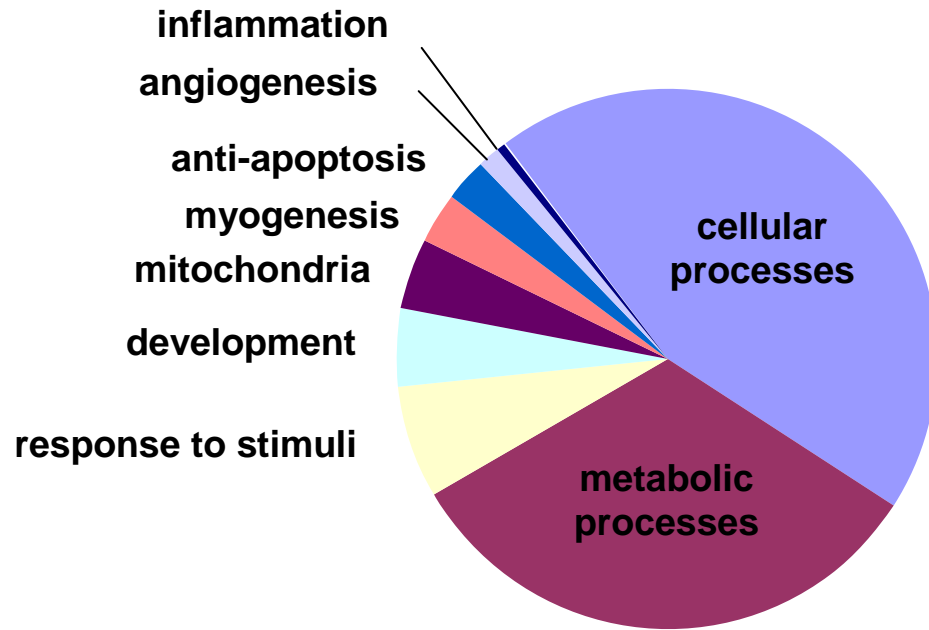


Figure 2.3: GO analysis of up-regulated genes in TG compared to WT in response to acute thermal injury.



Table 2.1: List of notable up-regulated genes in injured TG compared to WT from microarray analyses of 3 days post injury TA.

Locus	Name/description	Fold change
<b>Inflammation/chemotaxis</b>		
CCL2	Chemokine (C-C motif) ligand 2	3.425
IL10	Interleukin 10	1.408
IL1 $\beta$	Interleukin 1 $\beta$	4.42
TNF $\alpha$	Tumor necrosis factor	1.679
CD68	CD68 antigen	16.799
<b>Oxidative stress defense</b>		
Txn1	Thioredoxin 1	2.44
MT1	Metallothionein 1	2.352
MT2	Metallothionein 2	1.431
<b>Extracellular matrix</b>		
MMP2	Matrix metalloproteinase 2	1.58
MMP9	Matrix metalloproteinase 9	1.778
<b>Myogenic factors</b>		
Myh8	Myosin, heavy peptide, perinatal	17.766
MyoD	Myogenic differentiation	8.641
Myog	Myogenin	12.807

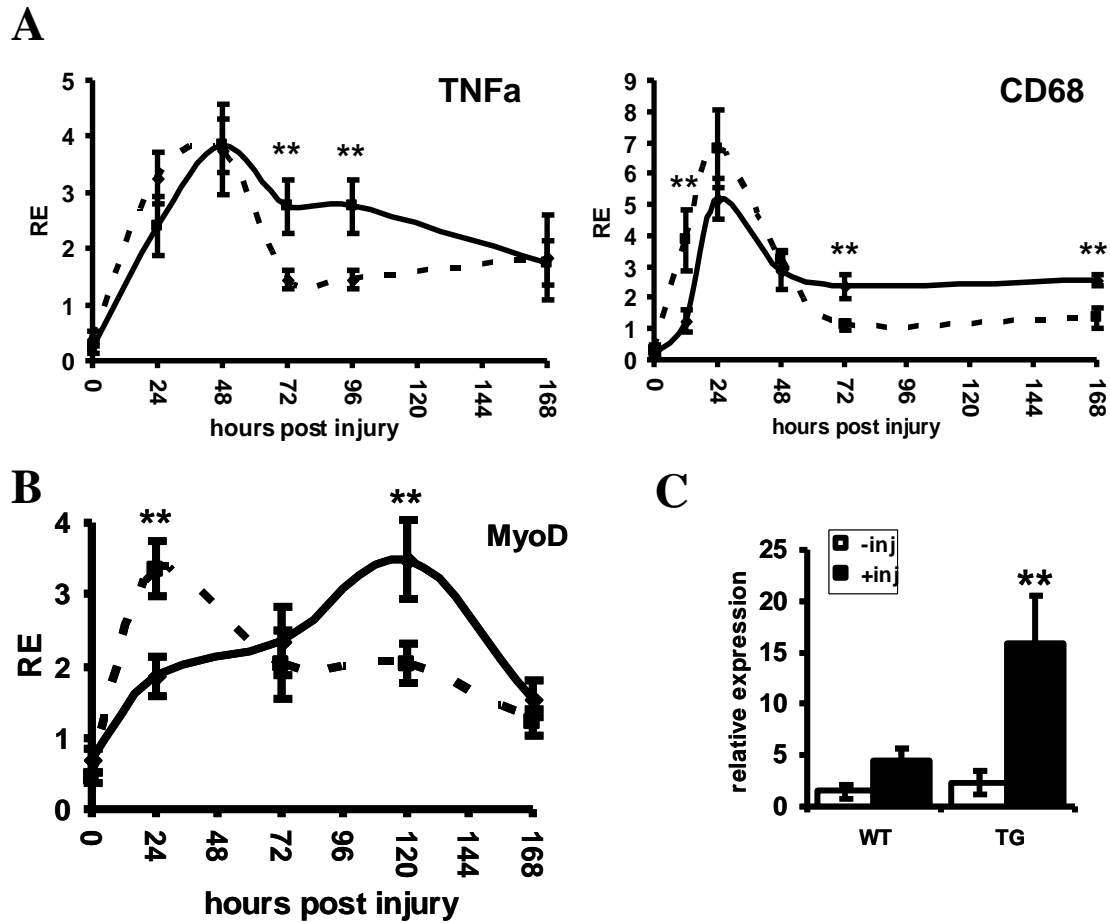


Figure 2.4: PPAR $\delta$  activation leads to temporal shift, thus increased efficiency, of the regenerative process. A) Temporal gene expression profiles of inflammatory (TNF $\alpha$  and CD68) and B) myogenic (MyoD) markers in response to injury measured by Q-PCR. C) Myh8 mRNA level 7 days post injury.

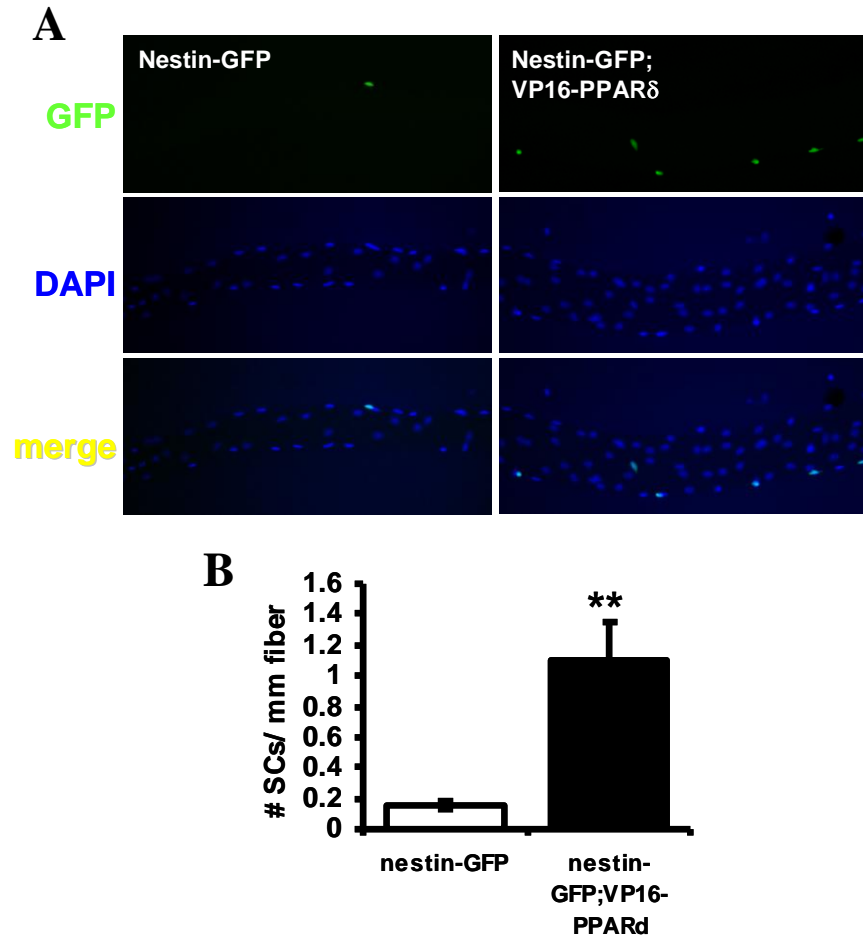


Figure 2.5: Muscle specific activation of PPAR $\delta$  increases quiescent satellite cell population. A) Visualization of quiescent satellite cells (+GFP) on isolated myofibers from lateral gastrocnemius of 8 wk old male mice. B) Quantification of GFP+ satellite cells per unit length of myofiber. C) QPCR on isolated nestin positive satellite cells from TG and WT animals.

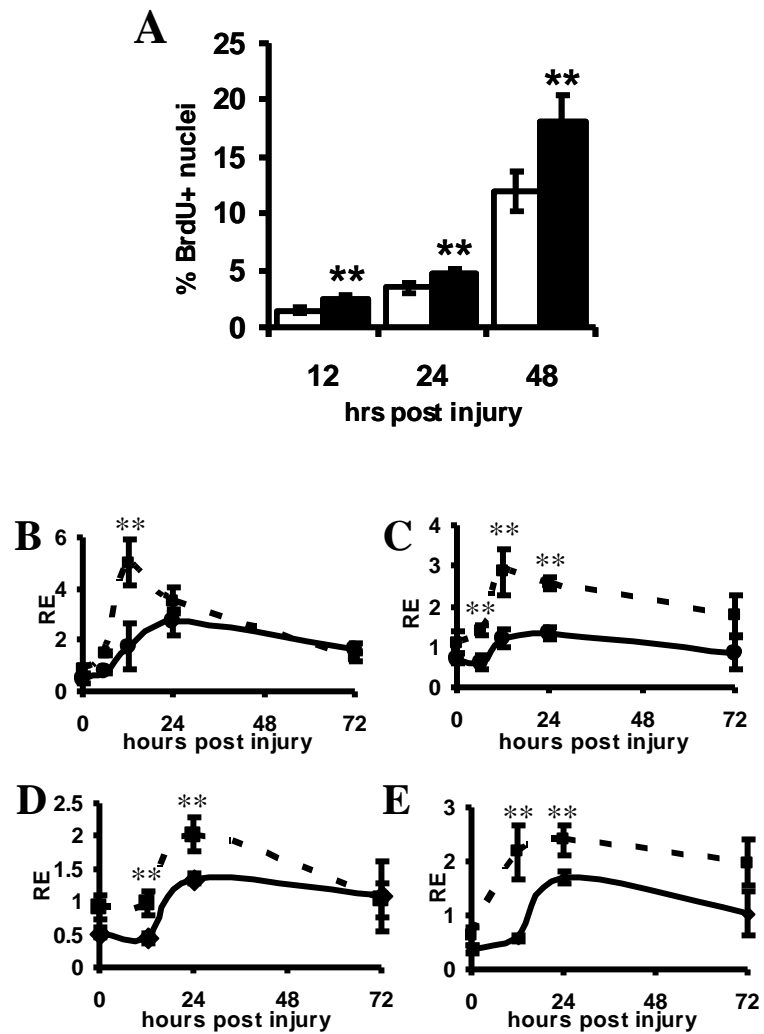


Figure 2.6: PPAR $\delta$  activation augments myoblast proliferation after the injury. A) Quantification of myogenic progenitor cell proliferation by BrdU incorporation after the injury. BrdU was injected once at 12, 24 or 48 hours after injury. TA was harvested 7 days after injury and BrdU staining was assessed against DAPI nuclear staining to calculate percentage of BrdU positive cells in total myonuclei per field. Temporal expression profile of Notch signaling pathway genes after the injury: B) Notch1 C) Hey1 D) Hes1 and E) Dll1.

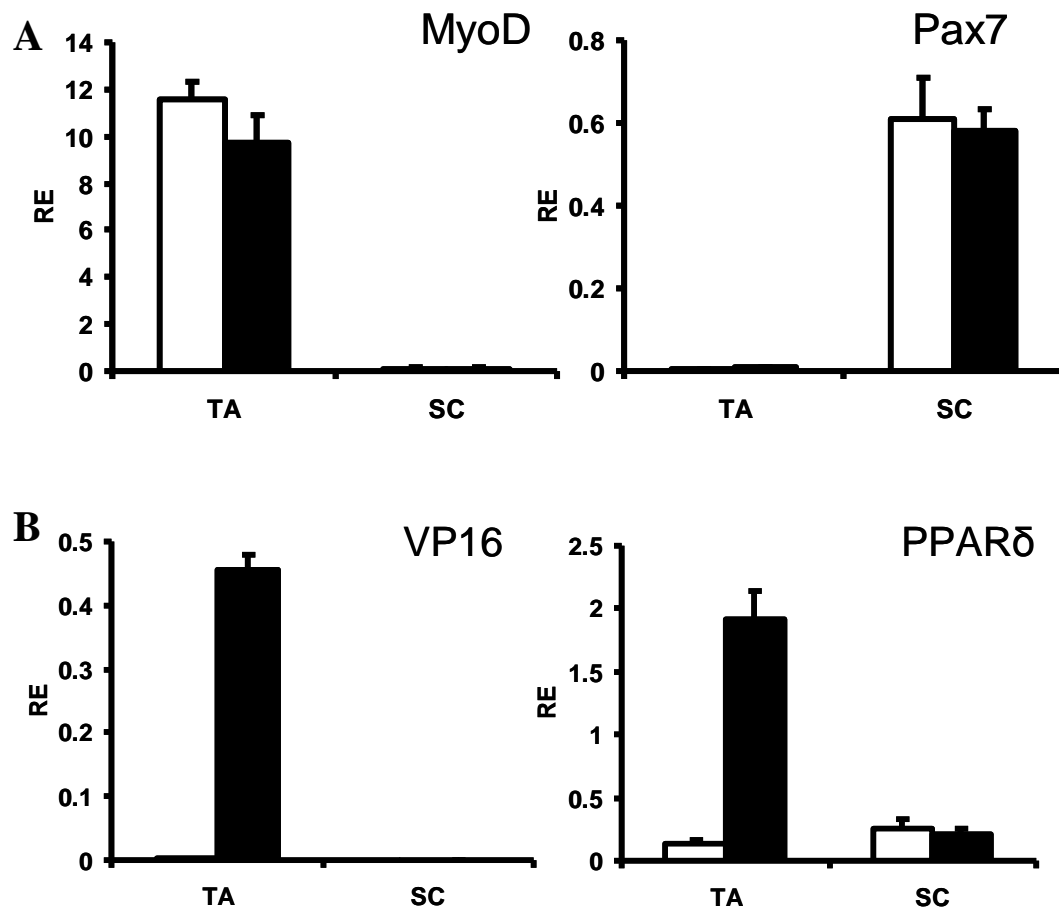


Figure 2.7: Transgene is not expressed in the satellite cells. Quiescent satellite cells were isolated and FACS sorted from nestin-GFP;VP16-PPAR $\delta$  double transgenic animals and gene expression was measured by QPCR. A) Isolated cells show absence of myogenic marker (MyoD) and presence of quiescent satellite cell marker (Pax7). B) The VP16 activation domain is absent, as a result, PPAR $\delta$  is not over-expressed in satellite cells.

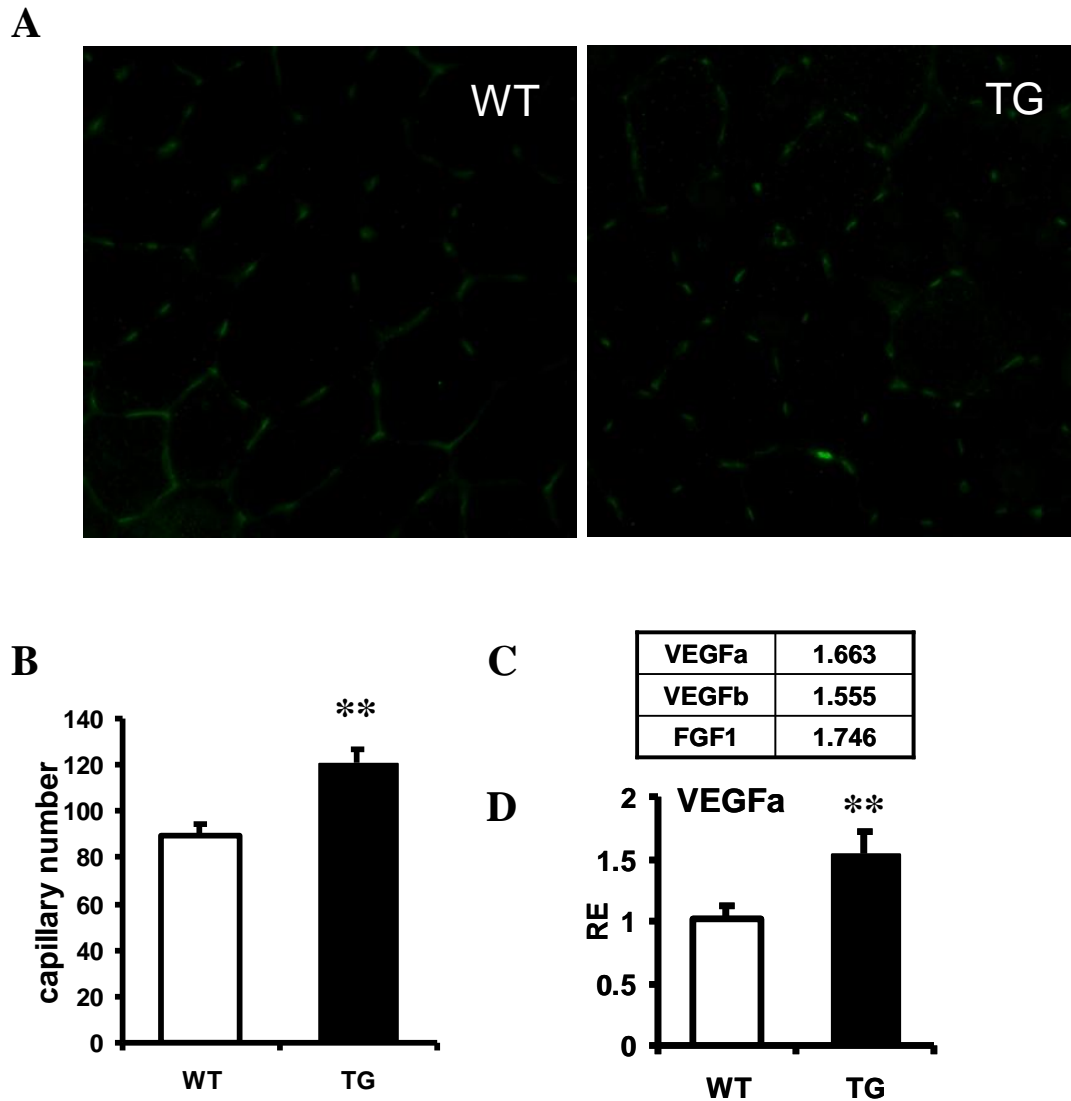


Figure 2.8: PPAR $\delta$  activation induces increase in vascularity. A) Immunostaining of transverse sections of TA from WT and TG animals for CD31. B) Quantification of CD31+ capillary number per field of view. C) Fold induction values of angiogenic genes from microarray comparing TG to WT. D) QPCR validation of VEGFa expression in TA.

## References

- Amthor H et al. (2009) Muscle hypertrophy driven by myostatin blockage does not require stem/precursor-cell activity. *PNAS* 106(18):7479-84.
- Angione AR, Jiang C, Pan D, Wang YX and S Kuang. PPAR $\delta$  regulates satellite cell proliferation and skeletal muscle regeneration. *Skelet Muscle*. 1(1):33, 2011.
- Arnold, L., Henry, A., Poron, F., Baba-Amer, Y., van Rooijen, N., Plonquet, A., Gherardi, R.K., and B. Chazaud. Inflammatory monocytes recruited after skeletal muscle injury switch into anti-inflammatory macrophages to support myogenesis. *J. Exp. Med.* 2007, 204(5): 1057-1069.
- Artvanis-Tsakonas S, Rand MD and RJ Lake. Notch signaling: cell fate control and signal integration in development. *Science*. 284(5415):770-6, 1999.
- Bischoff R. The satellite cell and muscle regeneration. In: Engel AG, Franzini-Armstrong C (eds). *Myology*, Vol 1. McGraw-Hill, Inc., New York, 1994.
- Blanco-Bose WE and HM Blau. Laminin-induced change in conformation of preexisting  $\alpha$ 7 $\beta$ 1 integrin signals secondary to myofiber formation. *Dev Biol*. 233(1):148-60, 2001.
- Blanpain C, lowry WE, Pasolli HA and E Fuchs. Canonical notch signaling functions as a commitment switch in the epidermal lineage. *Genes Dev*. 20(21):3022-35, 2006.
- Bogdanovich S, Krag TO, Barton ER, Morris LD, Whittemore LA, Ahima RS and TS Khurana. Functional involvement of dystrophic muscle by myostatin blockage. *Nature*. 420(6914):418-21, 2002.
- Brack AS, Conboy MJ, Roy S, Lee M, Kuo CJ, Keller C and TA Rando. Increased Wnt signaling during aging alters muscle stem cell fate and increases fibrosis. *Science*. 317(5839): 807-810, 2007.
- Brack AS, Conboy IM, Conboy MJ, Shen J, and TA Rando. A temporal switch from Notch to Wnt signaling in muscle stem cells is necessary for normal adult myogenesis. *Cell Stem Cell*, 2: 50-59, 2008.
- Brüning JC, Michael MD, Winnay JN, Hayashi T, Hörsch D, Accili D, Goodyear LJ, and Kahn CR. A muscle-specific insulin receptor knockout exhibits features of the metabolic syndrome of NIDDM without altering glucose tolerance. *Mol Cell*. 2: 559-569, 1998.

Cantini, M., Masimino, M.L., Rapizzi, E., Rossini, K., Cantini, C., Libera, L.D., and U. Carraro. Human satellite cells proliferation in vitro is regulated by autocrine secretion of IL-6 stimulated by a soluble factor(s) released by activated monocytes. *Biochem Biophys Res Comm.* 1995, 16: 49-53.

Cantini, M. and U. Carraro. Macrophage released factor stimulates selectively myogenic cells in primary muscle culture. *J. Neuropathol. Exp Neurol.* 1995a, 54: 121-128.

Cantini, M., Masimino, M.L., Rapizzi, E., Rossini, K., Cantini, C., Libera, L.D., and U. Carraro. Human satellite cells proliferation in vitro is regulated by autocrine secretion of IL-6 stimulated by a soluble factor(s) released by activated monocytes. *Biochem Biophys Res Comm.* 1995b, 16: 49-53.

Carvalho AJ, Hollett P and NH McKee. Recovery of synergistic skeletal muscle function following ischemia, *J. Surg. Res.* 59(5):527-533, 1995.

Chan RK, Austen JR., WG, Ibrahim S, Ding GY, Verna N, Hechtman HB, and FD Moore Jr. Reperfusion injury to skeletal muscle affects primarily type II muscle fibers. *J Surg Res.* 122:54-60, 2004.

Charge, S.B.P., and M.A. Rudnicki. Cellular and molecular regulation of muscle regeneration. *Physiol Rev.* 84:209-238, 2004.

Chazaud B, Sonnet C, Lafuste P, Guillaume B, Rimaniol AC, Poron F, Authier FJ, Dreyfus PA and RK Gherardi. Satellite cells attract monocytes and use macrophages as a support to escape apoptosis and enhance muscle growth. *JCB.*163(5):1133-1143, 2003.

Conboy IM, Conboy MJ, Smythe GM and TA Rando. Notch-mediated restoration of regenerative potential to aged muscle. *Science.* 30-2: 1575-1577, 2003.

Contreras-Shannon V, Ochoa O, Reyes-Reyna SM, Sun D, Michalek JE, Kuziel WA, McManus LM, and PK Shireman. Fat accumulation with altered inflammation and regeneration in skeletal muscle of CCR2<sup>-/-</sup> mice following ischemic injury. *Am J Physiol Cell Physiol.* 292:C953-967, 2007.

Day K, Shefer G, Richardson JB, Enikolopov G and Z Yablonka-Reuveni. Nestin-GFP reporter expression defines the quiescent state of skeletal muscle satellite cells. *Dev Biol.* 304(1): 246-259, 2007.

Fre S, Huyghe M, Mourikis P, Robine S, Louvard D and S Artavanis-Tsakonas. Notch signals control the fate of immature progenitor cells in the intestine. *Nature.* 435(7044):964-8, 2005.



Gardner VO, Caiozzo VJ, Long ST, Stoffel J, MxMaster WC and CA Prietto. Contractile properties of slow and fast muscle following tourniquet ischemia. *Am J Sports Med.* 12: 417-423, 1984.

Ge Y, Wu AL, Warnes C, Liu J, Zhang C, Kawasome H, Terada N, Boppart MD, Schoenherr CJ and J Chen. mTOR regulates skeletal muscle regeneration in vivo through kinase-dependent and kinase-independent mechanisms. *Am J Physiol Cell Physiol.* 297(6): C1434-1444, 2009.

Gibson MC and E Schultz. The distribution of satellite cells and their relationship to specific fiber types in soleus and extensor digitorum longus muscles. *Anat Rec.* 202(3):329-337, 1982.

Grounds MD and JK McGeachie. A model of myogenesis in vivo, derived from detailed autoradiographic studies of regenerating skeletal muscle, challenges the concept of quantal mitosis. *Cell Tissue Res.* 250:563-569, 1987.

Hamer PW, McGeachie JM, Davies MJ and MD Grounds. Evans Blue Dye as an in vivo marker of myofibre damage: optimizing parameters for detecting initial myofibre membrane permeability. *J Anat.* 200(Pt 1): 69-79, 2002.

Husmann I, Soulet L, Gautron J, Martelly I and D Barritault. Growth factors in skeletal muscle regeneration. *Cytokine Growth Factor Rev.* 7(3): 249-258, 1996.

Jennische E. Ischaemia-induced injury in glycogen-depleted skeletal muscle. Selective vulnerability of FG-fibers. *Acta Physiol Scand.* 125: 727-734, 1985.

Kalhovde JM, Jerkovic R, Sefland I, Cordonnier C, Calabria E, Schiaffino S, Lømo T. "Fast" and "slow" muscle fibres in hindlimb muscles of adult rats regenerate from intrinsically different satellite cells. *J Physiol.* 562(Pt 3):847-57, 2005.

Karpati G and MJ Molnar. "Muscle fibre regeneration in human skeletal muscle diseases." In: Schiaffino S, Partridge T (eds). *Skeletal muscle repair and regeneration.* Springer, Dordrecht, 2008.

Kelly A.M. Satellite cells and myofiber growth in the rat soleus and extensor digitorum longus muscles. *Dev Bio.* 65(1): 1-10, 1978.

Larsson, L. Muscle strength and speed of movement in relation to age and muscle morphology. *J Appl Physiol.* 46(3):451-6, 1979.

Lexell, J., C. C. Taylor, and M. Sjostrom. What is the cause of the ageing atrophy? Total number, size and proportion of different fiber types studied in whole vastus lateralis muscle from 15- to 83-year-old men. *J Neurol Sci.* 84:275-294, 1988.

Lexell, J. and D. Downham. What is the effect of ageing on type 2 muscle fibres? *J Neurol Sci.* 107:250-251, 1992.

Luquet S, Lopez-Soriano J, Holst D, Fredenrich A, Melki J, Rassoulzadegan M and PA Grimaldi. Peroxisome proliferator-activated receptor  $\delta$  controls muscle development and oxidative capability. *FASEB J.* 17(15): 2299-2301, 2003.

McCroskery S, Thomas M, Maxwell L, Sharma M and R Kambadur. Myostatin negatively regulates satellite cell activation and self-renewal. *J. Cell Biol.* 162(6): 1135-1147, 2003.

I.S. McLennan. Degenerating and regenerating skeletal muscles contain several subpopulations of macrophages with distinct spatial and temporal distributions. *J. Anat.* 1996, 188: 17-28.

Menetrey J, Kasemkijwattana C, Day CS, Bosch P, Vogt M, Fu FH, Moreland MS and J Huard. Growth factors improve muscle healing in vivo. *J Bone Joint Surg Br.* Jan; 82(1):131-7, 2000.

Mignone JL, Kukekov V, Chiang AS, Steindler D and G Enikolopov. Neural stem and progenitor cells in nestin-GFP transgenic mice. *J Comp Neurol.* 469(3): 311-324, 2004.

Mizonoya W, Wakamatsu J, Tatsumi R, and Y Ikeuchi. Protocol for high-resolution separation of rodent myosin heavy chain isoforms in a mini-gel electrophoresis system. *Anal Biochem.* 377(1):111-3, 2008.

Moss, F.P. and C.P. Leblond. Satellite cell as the source of nuclei in muscle of growing rats. *Anat. Rec.* 1970, 170: 421-436.

Mourikis P, Sambasivan R, Castel D, Rocheteau P, Bizzarro V and S Tajbakhsh S. A Critical requirement for Notch signaling in maintenance of the quiescent skeletal muscle stem cell state. *Stem Cells.* Doi:10.1002/stem.775, 2011.

Musaro A, McCullagh K, Paul A, Houghton L, Dobrowolny G, Molinaro M, Barton ER, Sweeney HL and N Rosenthal. Localized IGF-I transgene expression sustains hypertrophy and regeneration in senescent skeletal muscle. *Nat Genet* 27:195–200, 2001.

Pimorady-Esfahani, A., Grounds, M.D., and P.G. McMenamin. Macrophages and dendritic cells in normal and regenerating murine skeletal muscle. *Muscle Nerve.* 1997, 20: 158-166.

Robertson, T.A., Maley, M.A.L., Grounds, M.D., and J.M. Papadimitriou. The role of macrophages in skeletal muscle regeneration with particular reference to chemotaxis. *Exp. Cell Res.* 1993, 207:321-331.

Rosenblatt JD, Lunt AI, Parry DJ and TA Partridge. Culturing satellite cells from living single muscle fiber explants. *In Vitro Cell Dev Biol Anim.* 31(10):773-9, 1995.

Schmalbruch H and U Hellhammer. The number of nuclei in adult rat muscles with special reference to satellite cells. *Anat Rec.* 189:169-176, 1977.

Schultz E, Gibson MC and T Champion. Satellite cells are mitotically quiescent in mature mouse muscle: an EM and radioautographic study. *J Exp Zool.* 206(3):451-6, 1978.

Schuster-Gossler K, Cordes R and A Gossler. Premature myogenic differentiation and depletion of progenitor cells cause severe muscle hypotrophy in Delta1 mutants. *PNAS.* 104(2):537-42, 2007.

Segawa M, Fukada S, Yamamoto Y, Yahagi H, Kanematsu M, Sato M, Ito T, Uezumi A, Hayashi S, Miyagoe-Suzuki Y, Takeda S, Tsujikawa K and H Yamamoto. Suppression of macrophage functions impairs skeletal muscle regeneration with severe fibrosis. *Exp Cell Res.* 314(17): 3232-3244, 2008.

Shefer G, Rauner G, Yablonka-Reuveni Z and D. Benayahu. Reduced satellite cell numbers and myogenic capacity in aging can be alleviated by endurance exercise. *PLoS One.* 5(10): e13307, 2010.

Snow, M.H. An autoradiographic study of satellite cell differentiation into regenerating myotubes following transplantation of muscles in young rats. *Cell Tissue Res.* 1978, 186(3):535-40.

Summan M, McKinstry M, Warren GL, Hulderman T, Mishra D, Brumbaugh K, Luster MI and PP Simeonova. Inflammatory mediators and skeletal muscle injury: a DNA microarray analysis. *J Interferon Cytokine Res.* 23(5): 237-245, 2003.

Summan M, Warren GL, Mercer RR, Chapman R, Hulderman T, van Rooijen N and PP Simeonova. Macrophages and skeletal muscle regeneration: a clodronate-containing liposome depletion study. *Am J Physiol Regul Integr Comp Physiol.* 290:R1488-R1495, 2006.

Teixeira CF, Zamuner SR, Zuliani JP, Fernandes CM, Cruz-Hofling MA, Fernandes I, Chaves F and JM Gutierrez. Neutrophils do not contribute to local tissue damage, but play a key role in skeletal muscle regeneration in mice injected with Bothrops asper snake venom. *Muscle Nerve.* 28(4):449-459, 2003.

Tidball J.G. and M. Wehling-Henricks. Macrophages promote muscle membrane repair and muscle fiber growth and regeneration during modified muscle loading in mice *in vivo.* *J. Physiol.* 2007, 578: 327-336.

J.G. Tidball. Inflammatory processes in muscle injury and repair. *Am J Physiol Regul Integr Comp Physiol*, 288: R345-353, 2005.

Vasyutina E, Lenhard DC, Wende H, Erdmann B, Epstein JA and C Birchmeier. RBP-J (Rbpsi) is essential to maintain muscle progenitor cells and to generate satellite cells. *PNAS*. 104(11):4443-8, 2007.

Verdijk, L. B., R. Koopman, G. Schaart, K. Meijer, H. H. Savelberg, and L. J. van Loon. Satellite cell content is specifically reduced in type II skeletal muscle fibers in the elderly. *Am J Physiol Endocrinol Metab*. 292:E151-157, 2007.

Wagner KR, McPherron AC, Winik N, Lee SJ (2002) Loss of myostatin attenuates severity of muscular dystrophy in mdx mice. *Ann Neurol* 52(6): 832-6.

Walters TJ, Ktagh JF and DG Baer. Influence of fiber-type composition on recovery from tourniquet-induced skeletal muscle ischemia-reperfusion injury. *Appl Physiol Nutri Metab*. 33:272-281, 2008.

Wang YX, Lee CH, Tjep S, Yu RT, Ham Y, Kang H and RM Evans. Peroxisome proliferator-activated receptor  $\delta$  activates fat metabolism to prevent obesity. *Cell*, 113: 159-170, 2003.

Wang YX, Zhang CL, Yu RT, Cho HK, Nelson MC, Bayuga-Ocampo CR, Ham J, Kang H and RM Evans. Regulation of muscle fiber type and running endurance by PPAR $\delta$ . *PLoS Biol*. 2(10):e294, 2004. Erratum in: *PLoS Biol*. 2005 Jan;3(1):e61.

Warren GL, O'Farrell L, Summan M, Hulderman T, Mishra D, Luster MI, Kuziel WA and PP Simeonova. Role of CC chemokines in skeletal muscle functional restoration after injury. *Am J Physiol Cell Physiol*. 286(5):C1031-1036, 2004.

Woitasko MD and RJ McCarter. Effects of fiber type on ischemia-reperfusion injury in mouse skeletal muscle, *Plast. Reconstr. Surg*. 102 (6): 2052-2063, 1998.

Yahiaoui L, Gvozdic D, Danialou G, Mack M, and BJ Petrof. CC family chemokines directly regulate myoblast responses to skeletal muscle injury. *J Physiol*. 586:3991-4004, 2008.

Zammit PS, Heslop L, Hudon V, Rosenblatt JD, Tajbakhsh S, Buckingham ME, Beauchamp JR and Partridge TA. Kinetics of myoblast proliferation show that resident satellite cells are competent to fully regenerate skeletal muscle fibers. *Exp Cell Res*. 281:39-49, 2002.

Zacks SI and MF Sheff. Age-related impeded regeneration of mouse minced anterior tibial muscle. *Muscle Nerve*. 5:152-161, 1982.

Zimowska M, Szczepankowska D, Streminska W, Papy D, Touraire MC, Gautron J, Barritault D, Moraczewski J and I Martelly. Heparan sulfate mimetics modulate calpain activity during rat soleus muscle regeneration. 188(2):178-87, 2001.

**Chapter 3:**  
**Effects of pharmacological activation of  
PPARdelta during skeletal muscle regeneration  
after acute injury**

## **Abstract**

Commercially available synthetic ligands make PPAR $\delta$  an ideal target for pharmacological manipulation. Activation by oral administration of PPAR $\delta$  specific ligand, GW501516, has been shown to mimic genetic activation of the receptor in many ways (Narkar, 2008; Tanaka, 2003). Therefore, we wondered if acute activation of PPAR $\delta$  by orally administered GW501516 can also confer benefits during skeletal muscle regeneration after acute thermal injury. We found that acute treatment with GW501516 is sufficient to promote efficient restoration of fiber integrity after the injury. Acute activation of PPAR $\delta$  reduces expression of inflammatory genes and increases BrdU positive cells 48 hours after the injury. Collectively, we demonstrate PPAR $\delta$  as a possible pharmacological target in treatment of acute muscle injury.

## Introduction

Potent PPAR $\delta$  specific agonist, GW501516, was developed by GlaxoSmithKline through combinatorial chemistry and structure based drug design (Figure 3.1). It is highly selective for human and also murine PPAR $\delta$ , 125 times against murine PPAR $\alpha$  and 50 times against murine PPAR $\gamma$  (Sznajdman, 2003). Its physiological activity was confirmed in vivo by dosing insulin-resistant middle-aged obese rhesus monkeys. GW501516 caused dose-dependent rise in serum HDL cholesterol while lowering LDL, fasting triglycerides, and fasting insulin (Oliver, 2001).

In skeletal muscle, administration of GW501516 ameliorated diet-induced weight gain and insulin resistance, specifically characterized by an enhanced metabolic rate and fatty acid beta-oxidation, mitochondria biogenesis and a reduction of intramuscular lipid droplets (Tanaka, 2003). Combined with exercise training regimen, GW501516 treatment increased oxidative fibers in gastrocnemius and enhanced endurance running capacity (Narkar, 2008).

We herein present PPAR $\delta$  as a possible therapeutic target to promote muscle regeneration after an acute injury. We found that the pharmacological activation of PPAR $\delta$  promotes restoration of fiber integrity. Acute PPAR $\delta$  activation facilitates suppression of inflammatory genes in the muscle shortly after the injury. Additionally, PPAR $\delta$  ligand treatment supports proliferation of myoblasts after the injury.



Collectively, we show that acute pharmacological activation of PPAR $\delta$  is sufficient to confer beneficial effects on regenerative process after an acute injury.

## **Materials and Methods**

### **Animals**

GW1516 was administered either by oral gavage or feed to 8 week old male C57BL6J mice (Jackson Laboratories). 5mg per kg of body weight per day of GW1516 was dissolved in DMSO and delivered in total volume of 200 ul of 0.5% carboxymethyl cellulose to each animal. Vehicle treated animals were given equal volume of DMSO and 0.5% carboxymethyl cellulose without the drug. Alternatively, animals were ad lib fed with regular rodent chow infused with 40mg/kg GW1516 or drug-free control chow (Harlan).

### **Freeze burn injury**

Tibialis anterior muscles were injured according to previously published methods with a few modifications (Brack, 2007). The animals were anesthetized by Isofurane inhalation during the procedure. The skin was shaved over the TA muscles on both legs and the area was cleaned with 100% isopropynol. A small incision was made on the skin to expose the TA muscle. On the control leg, the incision was mended without further treatment. On the experimental leg, a stainless-steel 1g weight equilibrated to the temperature of dry ice was placed directly on the exposed TA for 10 seconds. Following the thermal injury, incision was closed using VetBond. All injury procedures were performed on the left leg, and the right leg was used as control. The injured portion of the muscle was carefully removed for gene expression analyses.

## **Histology**

Animals were perfused with 15 ml of ice-cold PBS followed immediately by 20 ml of 10% saline buffered formalin (Fisher). Tibialis anterior muscles were excised and immersed in 4% paraformaldehyde (EMB) for at least 48 hours at 4°C. Tissues were washed thrice in PBS for 10 minutes each, at room temperature with gentle rocking. Tissues were sequentially dehydrated in the following order: 25%, 50%, 75%, 95% and 100% ethanol, 20 minutes each with two changes of solution at each concentration for the total of 40 minutes in each concentration. Finally, tissues were cleared in three changes of xylene at 10 minutes each. Xylene was replaced by paraffin for a few hours at 60°C then changed to fresh paraffin to let it permeate through the tissues over night. Tissues were then embedded in plastic molds.

Paraffin embedded tissue blocks were sectioned at 7 um thick on Leica Jung 2500 Microtome. 3-5 sections were acquired per step, 2 slides per step and each step was separated by 200 um. One slide from each step was H&E stained, on average 10 slides per animal, where “step” with the largest injury area was deemed as the center of the injury and used for analyses. For H&E staining, sections were de-paraffinized and rehydrated by submerging in the following: 3x xylene, 3 minutes each; 2x 100%, 90%, 75% ethanol for 2 minutes each; 50% ethanol for 2 minutes and ddH<sub>2</sub>O for 2 minutes. Slides were then stained in 50/50 Gill’s No2 Hematoxylin/H<sub>2</sub>O mixture. After 5 minutes, slides were placed under running tap water for 5 minutes and dehydrated in the following sequence: 50%, 75% and 95% ethanol for 2 minutes each. Slides were counter stained in 1% eosin (1% eosin Y in 95% ethanol with 500ul

glacial acetic acid) solution for 2 minutes. Slides then underwent two changes of 100% EtOH for 2 minutes each. Finally, they were cleared in three changes of xylene at 5 minutes each. Slides were dried under the fume hood and mounted with Entellen mounting media.

Three random non-overlapping fields were photographed for analysis. Regenerating fiber number was measured by counting the number of discernible muscle fibers with centralized myonuclei (Ge, 2009). Regenerating fiber cross sectional area (CSA) was measured using Image J software.

### **BrdU staining**

50mg/kg body weight of BrdU (Sigma) was injected intraperitoneally as solution of 10mg/ml BrdU in saline, either at 12, 24 or 48 hours after the freeze burn injury. TA muscles were harvested at 7 days after injury and processed for paraffin sections as described above. BrdU incorporation was visualized using the BrdU Labeling and Detection Kit I (Roche) and the slides were mounted with Vectashield with DAPI (Vector Labs).

### **Evans Blue dye staining**

Injured animals were injected with Evans Blue dye according published protocol (Hamer, 2002). Sterile 1% w/v Evans Blue dye in PBS was intraperitoneally injected at 1% volume relative to the animal's body mass. 7 hours after the injection, injured TA muscles were harvested. TA muscles were placed on a mound formed by mixing gum tragacanth with O.C.T. compound and snap-frozen by isopentane quenching in liquid nitrogen. The frozen tissues were stored at -80°C. Frozen

sections were cut in 10 $\mu$ m thickness and dried at room temperature for at least 1 hour. Sections were then fixed in ice-cold acetone for 2 minutes, air dried and quickly dipped in xylene. Dehydrated sections were mounted under coverslips with DPX. Sections were analyzed with the Rhodamine channel setting of the Leica fluorescent microscope. Amount of staining was measured by ImageJ software.

### **RT-QPCR**

Whole or partial tissues were homogenized by Polytron probe homogenizer in Trizol reagent (Invitrogen). 3ml of Trizol was used for up to 50mg of tissue and the homogenizer was set at level 5 and applied to the samples for 7 seconds. Total RNA was extracted from the homogenates according to the manufacturer's protocol with a few alterations: after the phases were separated, aqueous phase containing RNA was loaded onto the RNeasy Mini kit (Qiagen) to clean and isolate RNA according to the kit instructions. RNA concentrations were measured spectrophotometrically on NanoDrop 8000 (Thermo Scientific). 1 $\mu$ g of total RNA was reverse transcribed (RT) using Superscript II (Invitrogen) or iScript Reverse Transcription Supermix (BioRad) according to the respective manufacturer's instructions. cDNAs were diluted 1/40 with ddH<sub>2</sub>O and used as templates in RT-QPCR reactions with SYBRGreenER qPCR SuperMix detection system. qPCR reactions were performed on 7900HT Fast Real-Time PCR system (Applied Biosystems). Data were processed and analyzed using the SDS Software v2.4 (Applied Biosystems).

After isolation, satellite cells were FACS sorted for their GFP expression on BD FACSAria flow cytometer. Sorted cells were processed as above to isolate RNA,

except RNeasy Micro kit (Qiagen) was used to efficiently procure small amount of RNA. Isolated RNA was amplified using the WT Ovation RNA Amplification System (NuGEN) according to the manufacturer's protocol.

### **Primers**

Q-PCR primers were constructed by "Pick Primers" function on NCBI website for each gene. PPAR $\delta$  F:GCCTCGGGCTTCCACTAC, R: AGATCCGATCGCACT TCTCA; VP16 F: CGCTAGACGATTTTCGATCTGGAC, R: CGGTAAACATCTGCTCAAACCTCG; PDK4: 3'GCCATTATAAAGAAAGCAACTAAGCA, 5' CCAGAGACGCGTATTTCTACCA; CPT1 $\beta$ : 3'GGGTCCCAAAGTGGCCA, 5' CATGGGACTGGTCGATTGC; catalase F:AGCGACCAGATGAAGCAGTG, R: TCCGCTCTCTGTCAAAGTGTG; MYH8 F: CGTACGGTGTATCATTCCCAATG, R: TG GTGCAGGACCAGTTCGT; MCP1 F: GGCTCAGCCAGATGCAGTTAA, R: CCTACTCAT TGGGATCATCTTGCT.

### **Cryosection and immunofluorescence staining**

Frozen muscle tissues were transversely sectioned at 7-10  $\mu$ m thickness on Leica CM1850 cryostat. Sections were dried on slides at room temperature for at least 1 hour prior to storage at -80 °C.

For IF, slides were allowed to equilibrate to room temperature for at 15 minutes. If the sections were mounted in O.C.T., slides were washed twice in PBS for 3 minutes each to remove the mounting media. Sections were then fixed in pre-cooled 50/50 acetone/methanol mixture for 20 minutes at -20 °C. Slides were washed thrice

in PBS at room temperature for 2 minutes each to remove the fixative. Tissues were blocked in 10% goat serum (GS) for 1 hour at room temperature. Afterwards, tissues were incubated in primary antibody over night at 4 °C in humidified chamber. Excess antibody and loosely bound non-specific interactions were removed by three washes in 0.01% Tween-20/PBS at 5 minutes each. Sections were then incubated in appropriate secondary antibody at room temperature for 30 minutes. Slides were washed thrice in 0.01% Tween-20/PBS at 5 minutes each and mounted under coverslips with Vectashield with DAPI. Where appropriate, M.O.M. Fluorescein staining kit (Vector Labs) was used according to the manufacturer's instructions.

## Results

### *Acute pharmacological activation of PPAR $\delta$ confers regenerative advantage*

Previously, pharmacological activation of PPAR $\delta$  has been shown to induce PPAR $\delta$  target genes in fast-twitch hind limb muscles (Narkar, 2008). In order to test whether an acute pharmacological activation of PPAR $\delta$  can modulate regenerative process after an acute injury, C57BL6J mice were treated with GW101516 for 4 days prior to and 5 days after a thermal injury to the tibias anterior (TA) muscle. Up-regulation of known PPAR $\delta$  target genes was confirmed by QPCR, attesting to the successful delivery and activity of the PPAR $\delta$  ligand in the muscle (Figure 3.1).

While vehicle treated animals showed dye uptake in 7.56% of the cross sectional area (CSA), merely 4.94% of the muscle CSA was stained in the ligand treated animals (Figure 3.2). The drug treated animals showed 34.7% reduction in the proportion of stained area 5 days after the injury, demonstrating that pharmacological activation of PPAR $\delta$  enables accelerated restoration of myofiber integrity after the injury. When the drug was administered at the time of injury through tissue harvest 5 days later, we did not observe statistically significant changes in Evans Blue dye uptake, suggesting that pre-conditioning of the muscle prior to injury may be necessary to achieve regenerative advantage (data not shown).

### *GW501516 treatment promotes resolution of inflammatory response and proliferation of myoblasts*

Considering the anti-inflammatory effects of PPAR $\delta$  activation, and the results from genetic activation of PPAR $\delta$  during regeneration, we measured the expression of



inflammatory marker genes at 12 and 24 hours after the injury. While the initial inflammatory responses are similarly generated with or without the PPAR $\delta$  ligand treatment at 12 hours after the injury, by 48 hours after the injury, the expressions of inflammatory marker genes were significantly reduced by the PPAR $\delta$  agonist treatment (Figure 3.3).

GW 501516 has been shown to induce cell proliferation in vitro (Angione, 2011). Therefore, we sought to determine whether pharmacological activation of PPAR $\delta$  in vivo can elicit similar responses during regeneration. BrdU injection at 48 hours after the injury revealed that PPAR $\delta$  activation does promote myoblast proliferation after the injury (Figure 3.4). Lastly, we determined the activation of Notch signaling pathway in response to PPAR $\delta$  activation in uninjured Quadriceps after 9 days of ligand treatment. Interestingly, while Notch1 and its target genes, Hes1 and Foxo1, were induced by PPAR $\delta$  ligand treatment, Notch ligand, Delta1 was not induced. It is possible that endogenous level of Delta1 may be sufficient to up-regulate the signaling pathway if the Notch1 receptor level is induced (Figure 3.5). Curiously, activation of Notch signaling pathway was confirmed at 3 days after the injury in drug treated animals (data not shown). It is possible that Notch signaling had already been down regulated at the end of proliferative phase by day 3. Further analysis on time points immediately following the injury is necessary.

## Discussion

We herein present a novel role for pharmacological activation of PPAR $\delta$  by its synthetic agonist, GW501516, in muscle regeneration. The agonist treatment facilitates restoration of fiber integrity after an acute thermal injury. Molecularly, GW501516 reduces expression of inflammatory genes 48 hours after the injury. Strikingly, ligand treatment also increases the number of BrdU positive proliferating cells at 48 hours after the injury. Additionally, ligand treatment induces activation of Notch signaling pathway in the absence of injury, while same was not observed 3 days after the injury.

In this study, PPAR $\delta$  ligand was administered orally and delivered systemically for effects targeted to multiple cell types. Specifically, suppression of inflammatory genes after the injury may be directed by the PPAR $\delta$  activation in the macrophages (Barish, 2008). It has been shown that acute PPAR $\delta$  activation can rapidly induce angiogenesis in muscle, which may establish key infrastructure to support critical immune response after the injury (Gaudel, 2008). Moreover, GW501516 may be directly activating the receptor in satellite cells to enhance proliferative kinetics (Angione, 2011). Nonetheless, as a potential treatment for a complex, multi-phasic regenerative process, involving a variety of cell types, it may be necessary to target multiple components of the program to achieve beneficial effects.

Activation of Notch signaling pathway by the PPAR $\delta$  ligand may also be exploited for conditions in which decline in Notch signaling capacity leads to loss of muscle mass, such as in aging. Simply increasing the circulating Notch level is known

to rejuvenate satellite cell function in older animals (Conboy, 2003). It is of interest to administer PPAR $\delta$  ligand to older animals to observe the effects on regenerative capacity of the muscle. Of note, 4 weeks treatment with the GW ligand failed to induce an increase in the quiescent satellite cell number (data not shown). Since satellite cells do not undergo rapid turnover, length of ligand treatment may have been too short. Moreover, it is possible that an additional activation cue in the form of external stimuli may be required to initiate their exit from quiescence to proliferate. Nonetheless, GW treatment appears to promote myoblast proliferation in vivo after the injury, therefore, increased number of satellite cells is not required to expedite the regenerative process, but rather increased proliferative kinetics is sufficient.

Chapter 3, in parts, is currently being prepared for submission for publication. Embler, EK; Atkins, A; Downes, M; Evans RM. The dissertation author was the primary investigator and author of this material.

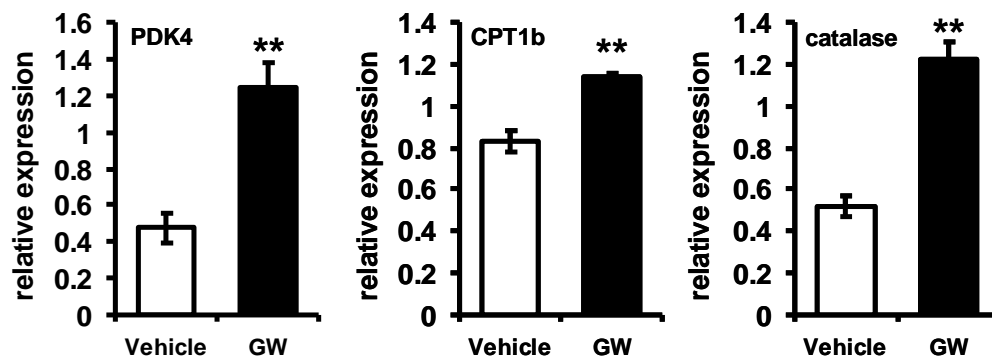


Figure 3.1: Oral administration of GW501516 induces expression of PPAR $\delta$  target genes in quadriceps. After 9 days of GW501516 treatment, RNA was harvested from quadriceps, reverse transcribed and subjected to RT-QPCR (+GW n=10; Vehicle n=6).

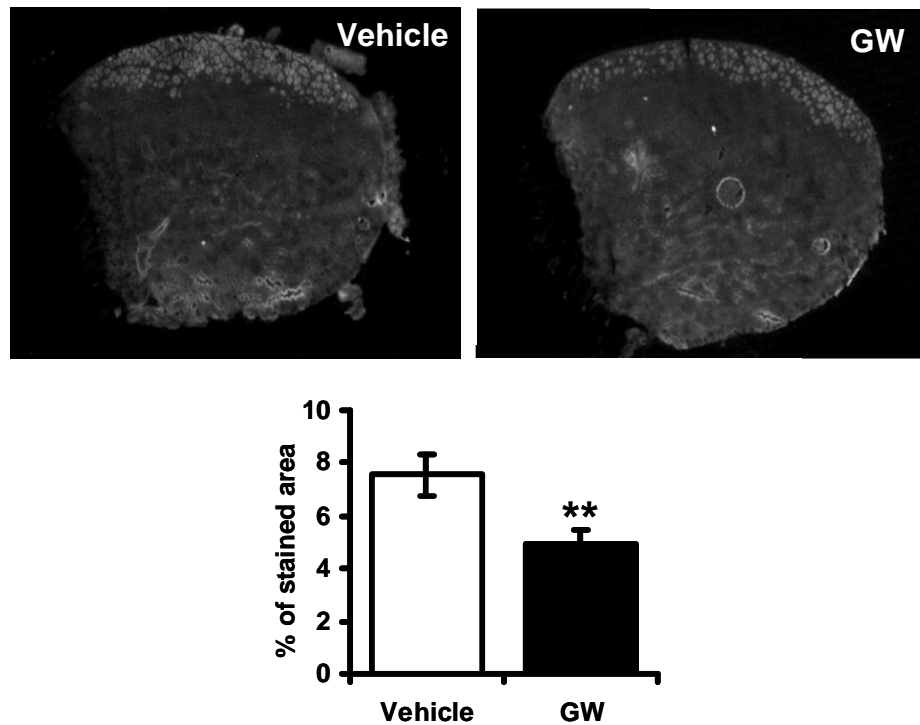


Figure 3.2: GW501516 treatment expedites restoration of fiber integrity after thermal injury. 8 week-old male C57BL6J animals were treated with GW501516 or vehicle only for 4 days prior to and 5 days after the injury (GW n=10; Vehicle n=6). 5 days after the injury, animals were injected intraperitoneally with Evans Blue dye. Proportions of stained area were calculated as percentage of stained to total cross sectional area of TA.

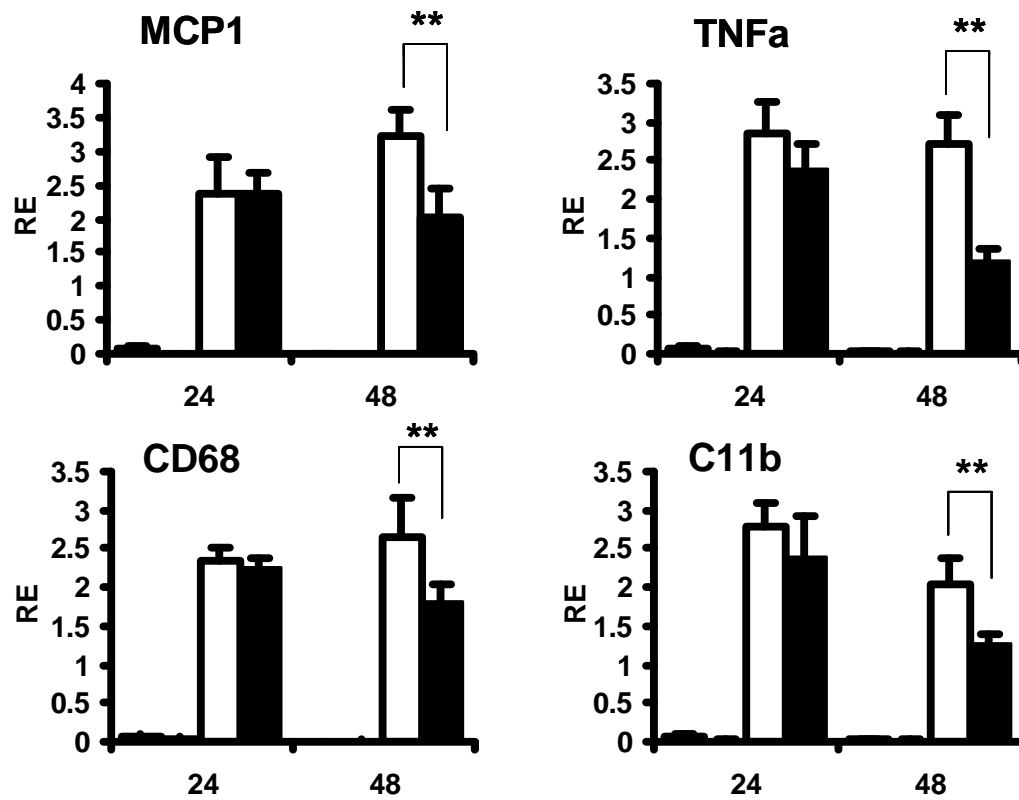


Figure 3.3: GW501516 treatment promotes resolution of inflammatory response. QPCR analysis for the expression of inflammatory markers, MCP1, TNF $\alpha$ , CD68 and CD11b at 24 and 48 hours after the injury.

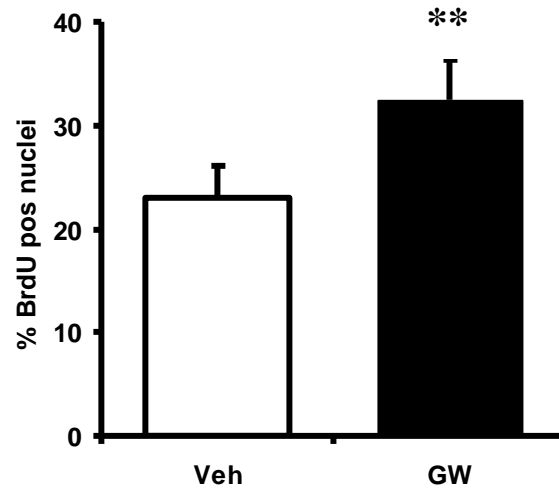


Figure 3.4: GW501516 treatment enhances proliferation of myoblasts after the injury. Proliferating cells were marked by incorporation of BrdU and weighted against total nuclei in a field. 2-3 random fields were chosen per animal, with n=4 for each genotype,  $p < 0.05$ .

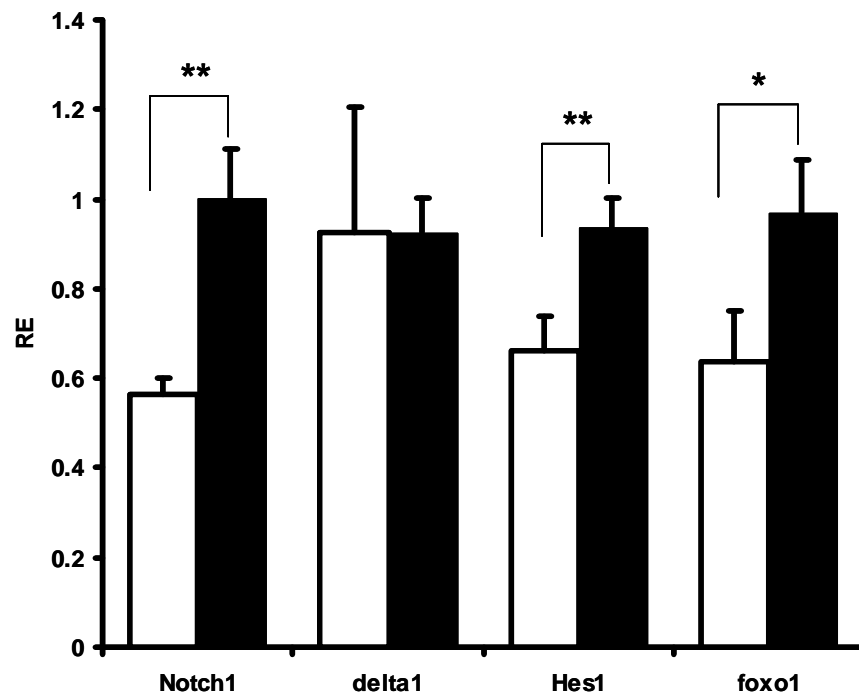


Figure 3.5: GW501516 treatment activates Notch1 signaling pathway. TA was harvested from C57BL6J animals treated with GW501516 for 9 days and processed for gene expression analysis by QPCR. White bar = vehicle treated; black bar = GW treated.



## References

- Brack AS, Conboy MJ, Roy S, Lee M, Kuo CJ, Keller C, Rando TA. Increased Wnt signaling during aging alters muscle stem cell fate and increases fibrosis. *Science*. 317(5839):807-10, 2007.
- Conboy IM, Conboy MJ, Smythe GM and TA Rando. Notch-mediated restoration of regenerative potential to aged muscle. *Science*. 30-2: 1575-1577, 2003.
- Gaudel C, Schwartz C, Giordano C, Abumrad NA and PA Grimaldi. Pharmacological activation of PPARbeta promotes rapid and calcineurin-dependent fiber remodeling and angiogenesis in mouse skeletal muscle. *Am J Physiol Endocrinol Metab*. 295(2):E297-304, 2008.
- Ge Y, Wu AL, Warnes C, Liu J, Zhang C, Kawasome H, Terada N, Boppart MD, Schoenherr CJ and J Chen. mTOR regulates skeletal muscle regeneration in vivo through kinase-dependent and kinase-independent mechanisms. *Am J Physiol Cell Physiol*. 297(6): C1434-1444, 2009.
- Hamer PW, McGeachie JM, Davies MJ and MD Grounds. Evans Blue Dye as an in vivo marker of myofibre damage: optimizing parameters for detecting initial myofibre membrane permeability. *J Anat*. 200(Pt 1): 69-79, 2002.
- Narkar VA, Downes M, Yu RT, Emblar E, Wang YX, Banayo E, Mihaylova MM, Nelson MC, Zou Y, Juguilon H, Kang H, Shaw RJ and RM Evans. AMPK and PPARdelta agonists are exercise mimetics. *Cell*. 134(3): 405-15, 2008.
- Oliver WR Jr, Shenk JL, Snaith MR, Russell CS, Plunket KD, Bodkin NL, Lewis MC, Winegar DA, Sznaidman ML, Lambert MH, Xu HE, Sternbach DD, Kliewer SA, Hansen BC and TM Willson. A selective peroxisome proliferator-activated receptor delta agonist promotes reverse cholesterol transport. *PNAS*. 98(9): 5306-11, 2001.
- Sznaidman ML, Haffner CD, Maloney PR, Fivush A, Chao E, Goreham D, Sierra ML, LeGrumelec C, Xu HE, Montana VG, Lambert MH, Willson TM, Oliver WR Jr and DD Sternbach. Novel selective small molecule agonists for peroxisome proliferator-activated receptor delta (PPARdelta)--synthesis and biological activity. *Bioorg Med Chem Lett*. 13(9): 1517-21, 2003.
- Tanaka T, Yamamoto J, Iwasaki S, Asaba H, Hamura H, Ikeda Y, Watanabe M, Magoori K, Ioka RX, Tachibana K, Watanabe Y, Uchiyama Y, Sumi K, Iguchi H, Ito S, Doi T, Hamakubo T, Naito M, Auwerx J, Yanagisawa M, Kodama T and J Sakai. Activation of peroxisome proliferator-activated receptor delta induces fatty acid beta-oxidation in skeletal muscle and attenuates metabolic syndrome. *PNAS*. 100(26): 15924-9, 2003.

# **Chapter 4:**

# **Conclusions**

In this study we report that both genetic and pharmacological activation of PPAR $\delta$  accelerates the muscle regenerative process after an acute injury. PPAR $\delta$  transgenic mice demonstrated both earlier resolution of the inflammatory response and earlier induction of myogenic markers, suggesting that PPAR $\delta$  actuates a temporal shift of the regenerative process. In the uninjured muscle, we found that constitutive PPAR $\delta$  activation lead to over 6 fold increase in the number of quiescent satellite cells. Consistently, we observed an increase in the number of proliferating cells after injury, and the accelerated formation of nascent regenerating fibers in PPAR $\delta$  transgenic mice. Importantly, the regenerative benefits of genetic over-expression of constitutively active PPAR $\delta$  was reproduced by acute administration of the PPAR $\delta$  specific ligand, GW501516, which also promotes efficient restoration of fiber integrity, resolution of inflammatory response and proliferation of myoblasts after injury. Collectively, our findings allude to the therapeutic potential of PPAR $\delta$ , to accelerate the recovery from acute muscle injury.

While regenerative advantage was achieved in both genetic and pharmacological models of PPAR $\delta$  activation, it is important to acknowledge the inherent differences in the modes of receptor activation. In the genetic mouse model, the transgene is driven by human skeletal  $\alpha$ -actin promoter, whose expression is limited to the mature myofiber. Moreover, endogenous skeletal  $\alpha$ -actin protein is detectable at 9 d.p.c., and as such, it is possible that the ectopic expression of PPAR $\delta$  may be exerting its effects during embryogenesis (Miniou, 1999). In the synthetic ligand model, the drug is ingested orally, thereby activating endogenous PPAR $\delta$  in a

variety of tissues and cell types. Therefore, it is possible that these two models are achieving the same physiological output via different mechanisms.

Interestingly, both genetic and pharmacological activation of PPAR $\delta$  seem to affect similar aspects of the regenerative program. Both models promoted resolution of inflammatory response. In the transgenic model, the effects originate from the muscle itself, possibly attributable to the increase in the production of myokine or other factors. Moreover, we have shown that PPAR $\delta$  activation leads to adaptive changes in the vasculature, which is known to facilitate introduction of non-myogenic cells to the muscle and transport of soluble factors. While in the GW treated animals, the effects could be directly attributable to the PPAR $\delta$  receptor activation on macrophages and other immune cells, as well as the muscle itself. Furthermore, PPAR $\delta$  mediated increase in the quiescent satellite cell pool, which was not observed in the acute ligand model, may be attributable to the effects of the transgene during embryogenic satellite cell specification process. Proliferation kinetics of the satellite cells harvested from the transgenic animals was not determined. However, it is of interest to see if and when the transgene is turned on, and at which point how it may affect the cell properties, including proliferation and differentiation kinetics and self-renewal potential. We can not exclude the possibility that the transgene expression in the mature fibers may be inducing some soluble factors upon injury to promote myoblast proliferation. Conversely, because we did not observe an increase in the satellite cell pool due to the ligand treatment, increased myoblast proliferation is likely due to the direct drug effect on those cells.

Lastly, activation of Notch signaling pathway is of great interest. Notch signaling has been shown to control cell proliferation and fates in various tissues (Artvanis-Tsakonas, 1999; Fre, 2005; Blanpain, 2006). Specifically in the muscle, Notch signaling confers anti-myogenic properties, where abrogation of the signaling pathway during development and regeneration leads to premature differentiation (Schuster-Gossler, 2007; Vasyutina, 2007; Coboy 2002). In aging muscle, decline in regenerative potential is attributed to loss of Notch signaling (Conboy, 2003; Conboy, 2005). In light of our findings, PPAR $\delta$  activation may be beneficial not only in expediting regenerative process in young adults but also in ameliorating aging induced decline in satellite cell function.

In this study, we have expanded our previous understanding of the role of PPAR $\delta$  in muscle physiology. We have shown that PPAR $\delta$  not only controls running endurance and metabolic parameters in the muscle, but also its regenerative program. PPAR $\delta$  activation affects multiple facets of the regenerative program, exerting comprehensive but transient effects to expedite the progress. Our findings suggest that PPAR $\delta$  should serve as a potential pharmacological target to enhance regenerative capacity of the muscle in injury and other degenerative conditions where satellite cell function is compromised. Subsequently, it is of great interest to test the efficacy of the drug in aging or disease models.

## References

- Artavanis-Tsakonas S, Rand MD and RJ Lake. Notch signaling: cell fate control and signal integration in development. *Science*. 284(5415):770-6, 1999.
- Blanpain C, lowry WE, Pasolli HA and E Fuchs. Canonical notch signaling functions as a commitment switch in the epidermal lineage. *Genes Dev*. 20(21):3022-35, 2006.
- Conboy IM, Rando TA. The regulation of Notch signaling controls satellite cell activation and cell fate determination in postnatal myogenesis. *Dev Cell*. 3(3):397-409, 2002.
- Conboy IM, Conboy MJ, Smythe GM and TA Rando. Notch-mediated restoration of regenerative potential to aged muscle. *Science*. 30-2: 1575-1577, 2003.
- Conboy IM, Conboy MJ, Wagers AJ, Girma ER, Weissman IL, Rando TA. Rejuvenation of aged progenitor cells by exposure to a young systemic environment. *Nature*. 433(7027):760-4, 2005.
- Fre S, Huyghe M, Mourikis P, Robine S, Louvard D and S Artavanis-Tsakonas. Notch signals control the fate of immature progenitor cells in the intestine. *Nature*. 435(7044):964-8, 2005.
- Miniou, P., Tiziano, D., Frugier, T., Roblot, N., Le Meur, M., and J. Melki. Gene targeting restricted to mouse striated muscle lineage. *Nuc Acids Res*. 27(19): e27, 1999.
- Schuster-Gossler K, Cordes R and A Gossler. Premature myogenic differentiation and depletion of progenitor cells cause severe muscle hypotrophy in Delta1 mutants. *PNAS*. 104(2):537-42, 2007.
- Vasyutina E, Lenhard DC, Wende H, Erdmann B, Epstein JA and C Birchmeier. RBP-J (Rbpsi) is essential to maintain muscle progenitor cells and to generate satellite cells. *PNAS*. 104(11):4443-8, 2007.